KikGR time-course data from destination tissues and the blood, we were able to determine the migration potential of specific cell populations. This approach provides new insights into cell migration in vivo and builds upon previous attempts to model monocyte tissue kinetics (14). In addition, Fucci mice provide a sensitive, real-time indication of progress through the cell cycle with no carryover of signal to daughter cells. Future studies might use the KikGR and Fucci approaches to investigate the relative contributions of BM and spleen monocytes in other inflammatory diseases.

Our findings highlight the importance of the BM as the primary hematopoietic tissue and monocyte reservoir in tumor-bearing mice. Targeting excessive monocytopoiesis in the BM of tumor-bearing mice may limit not only the supply of tumor-infiltrating monocytes but also the expansion of the spleen monocyte pool. Therapies that limit the number of monocytes and macrophages that are available to the tumor may improve the prognosis of patients with cancer.

Materials and Methods

Methods for cell preparation, flow cytometry, adoptive transfer, and in vitro migration assays are provided in *SI Materials and Methods*. The antibodies used for flow cytometry are listed in Table S2.

Animals. Male C57BL/6J wild-type mice (CD45.2$^+$) were purchased from CLEA Japan or Japan SLC. Rosa26$^{CAG::KikGR}$ knockin mice (C57BL/6 background), which express KikGR in all cell types, were generated at RIKEN. KikGR BM chimeras were generated by lethally irradiating 6-wk-old male C57BL/6J host mice with a split dose of 9.5 Gy (OM-150HT X-ray system; OHMiC), followed by i.v. injection with 5×10^6 syngeneic BM cells pooled from the femurs, tibias, and spines of Rosa26$^{CAG::KikGR}$ donors. Chimeras were used for tumor inoculation or experiments at least 5 wk after BM transfer, at which stage >99% chimerism was observed in monocytes from the BM, blood, and spleen. B6.SJL-*Ptprc*^{a} *Pepc*^{b}/BoyJ congenic mice (CD45.1$^+$) were purchased from The Jackson Laboratory. These mice were crossbred with C57BL/6J mice to generate CD45.1$^+$ CD45.2$^+$ mice for adoptive transfer experiments. Fucci double transgenic mice were generated by crossbreeding FucciG$_1$ (line no. 639) and FucciS/G$_2$/M (line no. 474) animals (obtained from A. Miyawaki, RIKEN BioResource Center, Tsukuba, Japan) as described previously (21). These mice express the fusion proteins mKO2-hCdt1(30/120) and mAG-hGem (1/110) under the CAG promoter; the no. 639 and no. 474 mouse lines were used to overcome the poor expression in hematopoietic cells that is observed in other Fucci lines (22). KikGR and Fucci mice were backcrossed to C57BL/6 mice for at least 10 generations before use. Mice were 6–12 wk of age (9–15 wk for BM chimeras) when used for tumor inoculation or experiments. All mice were bred and maintained under specific pathogen-free conditions in animal facilities at the University of Tokyo, and all animal procedures were approved by and conducted in accordance with the guidelines of the Animal Care Committee of the Graduate School of Medicine, the University of Tokyo.

Tumor Inoculation. The 3LL tumor cell line (a subclone of the C57BL mouse-derived Lewis lung carcinoma line) was obtained from F. Abe (Nihon Kayaku, Tokyo). Mice were anesthetized with sodium pentobarbital (50 mg/kg, i.p.), the fur around the inoculation site was shaved to improve tumor visualization, and a 50-μL suspension of 5×10^5 tumor cells was injected s.c. into the right flank. Tumor dimensions were measured using digital calipers, and tumor volume (in cubic millimeters) was estimated using the formula volume = length × (width)^2 × 0.5, which is derived from the formula for a prolate spheroid.

Photoconversion Surgery. Photoconversion procedures were adapted from methods developed previously (24–27) and are depicted in Fig. 1*A*. KikGR BM chimeras were anesthetized with isoflurane [1–3% (vol/vol) by inhalation], the fur around the spleen or left femur was shaved, and the skin disinfected with 70% (vol/vol) ethanol.

For spleen photoconversion, an ~1.5-cm horizontal incision was made in the skin on the left side of the abdomen, the spleen visualized, and an ~0.5-cm incision was made in the abdominal wall, through which the spleen was externalized gently. Two pieces of sterile aluminum foil (folded to remove sharp edges that might cause injury) were arranged on either side of the spleen, shielding the skin and abdominal cavity. The spleen was irradiated with violet light (three sides × 3 min, 150 mW/cm^2) using spot UV curing equipment (SP9-250VB; USHIO) fitted with a 436-nm g-line band-pass filter, fiber optic cable (SF101-NQ), and square lens (X057). Light intensity was measured with a UIT-250 digital photometer (UVD-S405 detector; USHIO), and light source distance was set accordingly. During irradiation of the visceral surfaces, the spleen was held in place with a piece of sterile nonadhesive plastic film, moistened with saline, which did not affect light transmission. After photoconversion, the spleen was replaced, the abdominal cavity was closed with 6–0 nylon suture, and the skin was closed with 9-mm wound clips.

For femur photoconversion, an ~1.5-cm vertical incision was made in the skin on the dorsal side of the left thigh, and jeweler's forceps were used to separate the vastus lateralis and biceps femoris muscles gently, exposing the femur. This approach minimized interference with the sciatic nerve and blood vessels running through the thigh. Bone reduction forceps were used to hold the muscle clear of the femur while it was irradiated with violet light (5 min, 500 mW/cm^2). After photoconversion, the muscle surrounding the femur was replaced, and the skin was closed with 9-mm wound clips. Throughout and after both photoconversion procedures the spleen and femur were irrigated with sterile saline solution. Surgery and photoconversion were conducted concurrently on different mice, allowing one mouse to be photoconverted every 10 min. Mice were allowed to recover on a heating mat (37 °C) and regained full mobility within 30 min.

Mice were subjected to either spleen or femur photoconversion, never both. Unconverted mice (no surgery, to calibrate flow cytometry gates) and 0-h group mice (killed before photoconversion by terminal cardiac puncture and cervical dislocation, to assess photoconversion efficiency) were included in each experiment. Although surgery itself induced acute leukocytosis (peaking within 3 h), sham photoconversion experiments (in which surgery was performed with or without irradiation) confirmed that exposure to violet light did not affect myeloid cell distribution, as is consistent with previous findings (25).

For in vitro photoconversion, single-cell suspensions of BM cells (2.5×10^6 cells in 100 μL in transparent microcentrifuge tubes) were irradiated with violet light (3 min, 150 mW/cm^2). Cells either were analyzed immediately or were incubated for 24 h in RPMI culture medium/10% FBS at 37 °C (5% CO_2 humidified atmosphere) before analysis. In vitro photoconversion efficiency was >99%.

Calculation of Migration Probability and Residence Time for Tumor-Infiltrating Monocytes. Monocytes enter the tumor from the blood and leave the tumor (by dying or by exiting back to the blood) at uniform rates. Accordingly, migration into and exit from the tumor can be described by the differential equation, $d(N_T r_T)/dt = N_B r_B p - N_T r_T/\tau$ (Eq. **1**). p (/h) represents the probability per unit time that a cell will migrate from the blood to the tumor (migration probability). The units of p are scalable such that, for example, $p = 0.60/h = 0.01/min$. τ (h) represents the average time that a cell remains in the tumor before dying or exiting (residence time). Changes in tumor monocyte number caused by in situ proliferation were assumed to be negligible based on the very low proportions of actively proliferating monocytes detected in the tumors of Fucci mice. r_B and r_T (expressed as a function of time) represent the proportion of KikRed$^+$ cells in the blood or tumor, respectively, within the population of interest (e.g., BM-pool monocytes). N_B and N_T represent the total number of monocytes (both KikGreen$^+$ and KikRed$^+$) in the blood or tumor, respectively, and are assumed to remain constant over the duration of each 24-h experiment (Table S1). Monocyte accumulation in the blood was modeled by the equation, $r_B(t) = a_B$ [exp $(-k_{B1}t)$ − exp$(-k_{B2}t)$] (Eq. **2**). After substituting Eq. **2** into Eq. **1** and taking $m = (N_B/N)p$ and $k = 1/\tau$, the solution of Eq. **1** under the initial condition $r_T(0) = 0$ gives $r_T(t) = a_B m\{[\exp(-k_{B1}t) - \exp(-kt)]/(k - k_{B1}) - [\exp(-k_{B2}t) - \exp(-kt)]/(k - k_{B2})\}$ (Eq. **3**). Eqs. **2** and **3** were fitted to blood and tumor data obtained from KikGR mouse photoconversion experiments using weighted least squares regression to obtain estimates for a_B, k_{B1}, k_{B2}, m, and k, with weights given by the reciprocal of the variance of each measurement. The SE associated with each of the estimated parameters was determined by the law of error propagation. Finally, m and k (± SE) were used to calculate p and τ (± SE). Calculations were performed using the statistical software R (version 3.0.1; www.r-project.org).

Data Analyses. Blood and BM cell numbers were adjusted to represent whole-body values based on the assumptions that the total blood volume of a mouse is 7% of its body weight and that a single mouse femur comprises 1/15 of total body BM cells (37). Photoconversion of 100% of myeloid cells in the femur or spleen was not possible by the procedures used in this study, and, unlike the spleen, a single femur represents only a fraction of the whole-body BM pool. To correct for differences in the extent of photoconversion of each myeloid cell pool, the proportion of KikRed$^+$ cells in each tissue was multiplied by 100/(% photoconversion efficiency) and, in mice undergoing femur photoconversion, by a factor of 15. Thus, KikGR data represent the contribution of the spleen or whole-body BM if all myeloid cells within these pools were photoconverted at time 0 h. The number of KikRed$^+$ cells was calculated by

multiplying the adjusted proportion of KikRed$^+$ cells in each tissue by mean cell counts from nonphotoconverted or 0-h group mice (Table S1), thus ensuring that results did not reflect acute fluctuations in total cell numbers following surgery. Because variations in tumor size might have influenced infiltration by KikRed$^+$ cells, tumor cell numbers were normalized by tumor weight, i.e., multiplication by (mean tumor weight for experiment)/(tumor weight for individual mouse). Finally, to correct for differences in the whole-body abundances of spleen-pool and BM-pool cells, which could account for differences in their redistribution after photoconversion, some data for KikRed$^+$ cell numbers also were expressed as a proportion of their respective source pool (% pool).

Statistics. Results are expressed as mean ± SEM for n independent observations, where n represents the number of individual mice in each treatment group per time point. All data are representative of results obtained in at least two independent experiments. Where appropriate, data were statistically analyzed using GraphPad Prism software (version 6.0b; GraphPad Software) as follows: two-tailed unpaired t test (Fucci percentage data, KikGR in vitro photoconversion data, and migration probability and residence time data); one-way ANOVA with Dunnett's posttest (wild-type mouse tumor kinetics data, adoptive transfer data); one-way ANOVA with Tukey posttest (Fucci mean fluorescence intensity data); two-way ANOVA with Sidak posttest (KikGR time-course data); and two-way ANOVA with Tukey posttest (Fucci cell number data). P values less than 0.05 were considered to be statistically significant.

ACKNOWLEDGMENTS. We thank A. Miyawaki and the RIKEN BioResource Center for providing FucciG_1 and FucciS/G_2/M mice; C. Kasahara and A. Hata for animal care; S. Aoki and S. Fujita for expert technical assistance; and I. Bertoncello for helpful discussions. This work was supported by the Japan Science and Technology Agency CREST program; Grants-in-Aid for Scientific Research (C) 25460491 (to S.U.) and (B) 25293113 (to K.M.) from the Japanese Ministry of Education, Culture, Sports, Science and Technology; an Australian Government Prime Minister's Australia Asia Endeavour Award (to F.H.W.S.); and an E & V Puzey Foundation Scholarship (to F.H.W.S.).

1. Hanahan D, Coussens LM (2012) Accessories to the crime: Functions of cells recruited to the tumor microenvironment. *Cancer Cell* 21(3):309–322.
2. Lewis CE, Pollard JW (2006) Distinct role of macrophages in different tumor microenvironments. *Cancer Res* 66(2):605–612.
3. Qian BZ, Pollard JW (2010) Macrophage diversity enhances tumor progression and metastasis. *Cell* 141(1):39–51.
4. Pollard JW (2004) Tumour-educated macrophages promote tumour progression and metastasis. *Nat Rev Cancer* 4(1):71–78.
5. Mantovani A, Allavena P, Sica A, Balkwill F (2008) Cancer-related inflammation. *Nature* 454(7203):436–444.
6. Wynn TA, Chawla A, Pollard JW (2013) Macrophage biology in development, homeostasis and disease. *Nature* 496(7446):445–455.
7. Luis TC, Killmann NM, Staal FJ (2012) Signal transduction pathways regulating hematopoietic stem cell biology: Introduction to a series of Spotlight Reviews. *Leukemia* 26(1):86–90.
8. Kim CH (2010) Homeostatic and pathogenic extramedullary hematopoiesis. *J Blood Med* 1:13–19.
9. O'Malley DP, et al. (2005) Morphologic and immunohistochemical evaluation of splenic hematopoietic proliferations in neoplastic and benign disorders. *Mod Pathol* 18(12):1550–1561.
10. Woodruff MF, Symes MO (1962) The significance of splenomegaly in tumour-bearing mice. *Br J Cancer* 16:120–130.
11. Young MR, Aquino S, Young ME (1989) Differential induction of hematopoiesis and immune suppressor cells in the bone marrow versus in the spleen by Lewis lung carcinoma variants. *J Leukoc Biol* 45(3):262–273.
12. Bronte V, et al. (2000) Identification of a CD11b(+)/Gr-1(+)/CD31(+) myeloid progenitor capable of activating or suppressing CD8(+) T cells. *Blood* 96(12):3838–3846.
13. Swirski FK, et al. (2009) Identification of splenic reservoir monocytes and their deployment to inflammatory sites. *Science* 325(5940):612–616.
14. Leuschner F, et al. (2012) Rapid monocyte kinetics in acute myocardial infarction are sustained by extramedullary monocytopoiesis. *J Exp Med* 209(1):123–137.
15. Dutta P, et al. (2012) Myocardial infarction accelerates atherosclerosis. *Nature* 487(7407):325–329.
16. Cortez-Retamozo V, et al. (2012) Origins of tumor-associated macrophages and neutrophils. *Proc Natl Acad Sci USA* 109(7):2491–2496.
17. Cortez-Retamozo V, et al. (2013) Angiotensin II drives the production of tumor-promoting macrophages. *Immunity* 38(2):296–308.
18. van Furth R, Cohn ZA (1968) The origin and kinetics of mononuclear phagocytes. *J Exp Med* 128(3):415–435.
19. Nowotschin S, Hadjantonakis AK (2009) Use of KikGR a photoconvertible green-to-red fluorescent protein for cell labeling and lineage analysis in ES cells and mouse embryos. *BMC Dev Biol* 9:49.
20. Tsutsui H, Karasawa S, Shimizu H, Nukina N, Miyawaki A (2005) Semi-rational engineering of a coral fluorescent protein into an efficient highlighter. *EMBO Rep* 6(3):233–238.
21. Sakaue-Sawano A, et al. (2008) Visualizing spatiotemporal dynamics of multicellular cell-cycle progression. *Cell* 132(3):487–498.
22. Tomura M, et al. (2013) Contrasting quiescent G_0 phase with mitotic cell cycling in the mouse immune system. *PLoS ONE* 8(9):e73801.
23. Sawanobori Y, et al. (2008) Chemokine-mediated rapid turnover of myeloid-derived suppressor cells in tumor-bearing mice. *Blood* 111(12):5457–5466.
24. Tomura M, et al. (2008) Monitoring cellular movement in vivo with photoconvertible fluorescence protein "Kaede" transgenic mice. *Proc Natl Acad Sci USA* 105(31):10871–10876.
25. Tomura M, et al. (2010) Activated regulatory T cells are the major T cell type emigrating from the skin during a cutaneous immune response in mice. *J Clin Invest* 120(3):883–893.
26. Kotani M, et al. (2013) Systemic circulation and bone recruitment of osteoclast precursors tracked by using fluorescent imaging techniques. *J Immunol* 190(2):605–612.
27. Tomura M, Kabashima K (2013) Analysis of cell movement between skin and other anatomical sites in vivo using photoconvertible fluorescent protein "Kaede"-transgenic mice. *Methods Mol Biol* 961:279–286.
28. Serbina NV, Hohl TM, Cherny M, Pamer EG (2009) Selective expansion of the monocytic lineage directed by bacterial infection. *J Immunol* 183(3):1900–1910.
29. Ugel S, et al. (2012) Immune tolerance to tumor antigens occurs in a specialized environment of the spleen. *Cell Rep* 2(3):628–639.
30. Hettinger J, et al. (2013) Origin of monocytes and macrophages in a committed progenitor. *Nat Immunol* 14(8):821–830.
31. Fogg DK, et al. (2006) A clonogenic bone marrow progenitor specific for macrophages and dendritic cells. *Science* 311(5757):83–87.
32. Marigo I, et al. (2010) Tumor-induced tolerance and immune suppression depend on the C/EBPbeta transcription factor. *Immunity* 32(6):790–802.
33. McAllister SS, et al. (2008) Systemic endocrine instigation of indolent tumor growth requires osteopontin. *Cell* 133(6):994–1005.
34. Sunderkötter C, et al. (2004) Subpopulations of mouse blood monocytes differ in maturation stage and inflammatory response. *J Immunol* 172(7):4410–4417.
35. Qian BZ, et al. (2011) CCL2 recruits inflammatory monocytes to facilitate breast-tumour metastasis. *Nature* 475(7355):222–225.
36. Serbina NV, Pamer EG (2006) Monocyte emigration from bone marrow during bacterial infection requires signals mediated by chemokine receptor CCR2. *Nat Immunol* 7(3):311–317.
37. Boggs DR (1984) The total marrow mass of the mouse: A simplified method of measurement. *Am J Hematol* 16(3):277–286.

Iinuma et al. Journal of Translational Medicine 2014, 12:84
http://www.translational-medicine.com/content/12/1/84

JOURNAL OF TRANSLATIONAL MEDICINE

RESEARCH Open Access

Phase I clinical study of multiple epitope peptide vaccine combined with chemoradiation therapy in esophageal cancer patients

Hisae Iinuma[1*], Ryoji Fukushima[1], Tsuyoshi Inaba[1], Junko Tamura[1], Taisuke Inoue[1], Etsushi Ogawa[1], Masahiro Horikawa[1], Yoshibumi Ikeda[1], Noriyuki Matsutani[1], Kazuyoshi Takeda[5], Koji Yoshida[2,3], Takuya Tsunoda[2,3], Tadashi Ikeda[1], Yusuke Nakamura[2,4] and Kota Okinaga[1]

Abstract

Background: Chemoradiation therapy (CRT) has been widely used for unresectable esophageal squamous cell carcinoma (ESCC) patients. However, many patients develop local recurrence after CRT. In this study, we hypothesized that the immunotherapy by peptide vaccine may be effective for the eradication of minimal residual cancer cells after CRT. This study was conducted as a phase I clinical trial of multiple-peptide vaccine therapy combined with CRT on patients with unresectable ESCC.

Patients and methods: HLA-A*2402 positive 11 unresectable chemo-naïve ESCC patients were treated by HLA-A*2402-restricted multi-peptide vaccine combined with CRT. The peptide vaccine included the 5 peptides as follows; TTK protein kinase (TTK), up-regulated lung cancer 10 (URLC10), insulin-like growth factor–II mRNA binding protein 3 (KOC1), vascular endothelial growth factor receptor 1 (VEGFR1) and 2 (VEGFR2). CRT consisted of radiotherapy (60 Gy) with concurrent cisplatin (40 mg/m^2) and 5-fluorouracil (400 mg/m^2). Peptide vaccines mixed with incomplete Freund's adjuvant were injected subcutaneously once a week on at least 8 occasions combined with CRT.

Results: Vaccination with CRT therapy was well-tolerated, and no severe adverse effects were observed. In the case of grade 3 toxicities, leucopenia, neutropenia, anemia and thrombocutopenia occurred in 54.5%, 27.3%, 27.3% and 9.1% of patients, respectively. Grade 1 local skin reactions in the injection sites of vaccination were observed in 81.8% of patients. The expressions of HLA class I, URLC10, TTK, KOC1, VEGFR1 and VEGFR2 antigens were observed in the tumor tissues of all patients. All patients showed peptide-specific cytotoxic T lymphocytes responses in at least one of the 5 kinds of peptide antigens during the vaccination. Six cases of complete response (CR) and 5 cases of progressive disease (PD) were observed after the 8th vaccination. The 4 CR patients who continued the peptide vaccination experienced long consistent CR for 2.0, 2.9 4.5 and 4.6 years.

Conclusions: A combination therapy of multi-peptide vaccine with CRT can successfully be performed with satisfactory levels of safety, and application of this combination therapy may be an effective treatment for patients with unresectable ESCC.

Trial registration: ClinicalTrial.gov, number NCT00632333.

Keywords: Cancer vaccine, Chemoradiation therapy, Esophageal cancer, CTL, Phase I clinical trial

* Correspondence: iinuma@med.teikyo-u.ac.jp
[1]Department of Surgery, Teikyo University School of Medicine, Tokyo, Japan
Full list of author information is available at the end of the article

Background

Esophageal squamous cell carcinoma (ESCC) is a highly malignant disease, especially in Asia. In Japan, the number of deaths attributable to ESCC has been slowly increasing, and 11,345 people died in 2011 [1]. Recent developments in surgical techniques and postoperative management including chemotherapy and fractionized radiation therapy, have contributed to improvements in the surgical outcome [2,3]. Chemoradiation therapy (CRT) has been used in Japan since 1990, especially for unresectable ESCC patients with locally advanced disease and/or distant metastasis, or for those who were not fit to undergo surgery [3]. However, it has been reported that many patients develop local recurrence soon after CRT [4-8]. This recurrence is due to the difficulty in making a precise clinical assessment of CRT on the treated cancer tissues. Viable cancer cells are thought to remain at the primary site in the majority of patients even if clinical complete response (CR) is accomplished. Although salvage esophagectomy was recommended in recurrent patients after CRT, high incidences of mortality and radiation-related post-operative complications, such as pneumonitis and cardiomyositis, have been reported [9]. Therefore, the development of a new approach for residual cancer cells after CRT is necessary to improve the prognosis of patients with unresectable ESCC.

A multimodality approach for ESCC is preferred in order to improve prognosis of CRT, and immunotherapy can be viewed as one rational approach for combination therapy with CRT. Recent studies have suggested that local irradiation elicits immunomodulatory effects and induces tumor-specific immune responses [10-14]. Furthermore, fluorouracil (5-FU) and cisplatin (CDDP), the standard agents for the treatment of ESCC, may immunomodulate the anti-tumor immunological response through the down regulation of immunosuppressive regulatory T cells and/ or increase the expression of MHC molecules [15-17]. In this study, we hypothesized that the CRT may act immunogenically, and immunotherapy with peptide vaccine may be effective for the eradication of residual cancer cells after CRT.

By using cDNA microarray technology coupled with laser microdisection, we identified novel HLA-A*2402 (which is the most common HLA-A allele in the Japanese population) - restricted epitope peptides as targets for cancer vaccination [18-21]. In particular, it has been demonstrated that TTK protein kinase (TTK), up-regulated lung cancer 10 (URLC10) and insulin-like growth factor–II mRNA binding protein 3 (KOC1) are promising targets for cancer vaccination in advanced ESCC patients [22,23]. Furthermore, to overcome the inhibition of the antitumor effects of cytotoxic T lymphocytes (CTL), which occur due to the down regulation of human leukocyte antigen (HLA), we focused on the peptide vaccine targeting the vascular endothelial growth factor receptor 1 (VEGFR1) and 2 (VEGFR2). It has been reported that CTLs were strongly induced by these peptides in various cancer patients [24].

In this study, we attempted a phase I clinical trial of multi-peptide vaccines in combination with CRT for unresectable ESCC patients. We selected 5 peptide vaccines (TTK, URLC10, KOC1, VEGFR1 and VEGFR2) to overcome the immune-escape mechanisms and increase the therapeutic potential of the cancer vaccine. The primary endpoint of this study is an evaluation of the safety factors, and secondary endpoints are estimation of the immune responses and clinical responses.

Materials and methods

Study design and treatment protocol

This study was a phase I clinical trial of dose-escalated multiple-peptide vaccine (TTK, URLC10, KOC1, VEGFR1 and VEGFR2) combined with CRT. Each peptide vaccine was mixed with incomplete Freund's adjuvant (IFA) (Montanide ISA 51; Seppic, Paris, France) separately, and was injected subcutaneously in 11 unresectable ESCC patients with stage II (3 cases), stage III (4 cases) or stage IV (4 cases). All patients were chemo-naïve. Treatment consisted of 2 courses of CDDP 40 mg/m^2 (day1, 8) and 5-FU 400 mg/m2/day (days 1-5, 8-12) combined with concurrent radiotherapy of 60 Gy in 30 fractions as described previously [7]. During the break period of chemotherapy, 5 kinds of peptide vaccines were administered once every week, a total 8 times (Additional file 1: Figure S1). Dose escalation was performed in 3 patients' cohort with dose of 0.5 mg, 1 mg and 3 mg for each peptide. For the imaging analysis, computed tomography (CT) scan and endoscopy were performed at pre-treatment period and every 2 ~ 3 months after the vaccination, and every measureable legion was evaluated by RECIST. CR patients additionally received 5 kinds of peptide vaccine, once every 2 weeks for 1 year and then once a month until changes to the progressive disease (PD) were observed. The primary endpoint of this trial was to evaluate the safety of this therapy. The secondary endpoints were to investigate the immunological response and clinical outcome. This study was approved by the Ethics Committee on Clinical Investigation of Teikyo University (Tokyo, Japan) and is registered with Clinical Trials.gov (NCT 00632333). Written informed consent was obtained from all individuals. The trial was carried out in accordance with the Helsinki declaration on experimentation on human subjects.

Patients eligibility

The eligibility criteria for patients participating in the clinical trial were as follows: (1) they were unresectable ESCC patients with widespread ESCC who refused

surgical resection, locally advanced or metastatic disease; (2) they have disease which is possible the evaluation of clinical response (no limitation with respect to the presence or absence of measurable diseases according to RECIST); (3) they were HLA-A*2402-positive patients by DNA typing of HLA-A genetic variations; (4) no therapy 4 weeks prior to the initiation of the trial; (5) ECOG performance status was 0-2; (6) their expected survival was at least 3 months; (7) the age of the patients was between >20 and <80 years; and (8) adequate bone-marrow, cardiac, pulmonary, hepatic and renal functions had to be present, including white blood cell count >2000/mm^3, platelet count >75000/mm^3, total bilirubin < 1.5 times of the institutional normal upper limits, creatinine < 1.5 times of the institutional normal upper limits, AST/ALT/ALP <2.5 times of the institutional normal upper limits. The exclusion criteria of patients participating in the clinical trial were as follows. (1) pregnancy; (2) breastfeeding; (3) active or uncontrolled infection; (4) concomitant treatment with steroids or immunosuppresing agents; (5) other active or uncontrolled other malignancy; (6) disease to the central nervous system; (7) some other form of unsuitableness as determined by the principal investigator or physician.

Toxicity assessment

Signs of toxicities were assessed by the Common Terminology Criteria for Adverse Event (CTCAE) version 3. Blood count and serum chemistry tests were performed every 2 weeks. The worst toxicity throughout the treatment period (2 courses of CRT and 8th peptide vaccination) was investigated. Dose escalation was performed in 3 patients' cohort with dose of 0.5 mg, 1 mg and 3 mg for each peptide. Dose-limiting toxicity (DLT) was defined as a hematological toxicity of grade 4 and non-hematological toxicity of grade 3 or greater.

Peptides

The peptides derived from TTK-567 (SYRNEIAYL), URLC10-177 (RYCNLEGPPI), KOC1-508 (KTVNELQNL), VEGFR1-1084 (SYGVLLWEIF), VEGFR2-169 (RFVPDG NRI) that bound to the HLA-A*24 molecule were synthesized by the American Peptide Company (Sunnyvale, CA, USA). The purity (>97%) and identify of the peptides were determined by analytical high-performance liquid chromatography (HPLC) and mass spectrometry analysis, respectively. The endotoxin levels and bioburden of these peptides were tested and determined to be within acceptable levels as GMP grade for the vaccines (NeoMPS, Inc.).

Measurement of CTL responses

An enzyme-linked immunospot (ELISPOT) assay was performed to measure the peptide specific CTL response, as described previously [23,25]. For the evaluation of CTL and Flow cytometry, blood samples were obtained from the patients at the pre-vaccination period and after the 4th, 8th, 12th and 16th vaccinations. Briefly, peripheral blood mononuclear cells (PBMCs) of blood samples were cultured with respective peptide and IL-2 (Novartis, Emeryville, CA) at 37°C for two weeks. Peptide was added into the culture at day 0 and day 7. Following CD4$^+$ cell depletion by Dynal CD4 positive isolation kit (Invitrogen, Carlsbad, CA), IFN-γ ELISPOT assay was performed using Human IFN-γ ELISPOT PLUS kit (MabTech, Nacka Strand, Sweden) according to the manufacturer's instructions. The number of peptide specific spots was calculated by subtracting the spot number in the control well from the spot number of wells with peptide-pulsed TISI cells. The positivity of the antigen-specific T cell responses were classified into four grades (−, +, ++ and +++), depending on the peptide-specific spots at different responder/stimulator ratios. When the algorithm indicated +, ++ or +++, we judged it to be a positive case.

Flow cytometry

Expression of peptide specific T cell receptors was analyzed on FACS-CantoII (Becton Dickinson,. San Jose, CA) using URLC10, TTK, KOC1, VEGFR1 or VEGFR2-derived epitope peptide-MHC dextramer (Immudex, Copenhagen, Denmark) or tetramer-PE (Medical & Biological Laboratories Co.,Ltd., Nagoya, Japan) according to the manufacturer's instructions. HIV-derived epitope peptide (RYLRDQQLL)-MHC dextramer or tetramer-PE was used as a negative control. T cells were incubated with peptide-MHC dextramer or tetramer-PE, treated with FITC-conjugated anti-human CD8 mAb, APC-conjugated anti-human CD3 mAb, PE-Cy7-conjugated anti-human CD4 mAb, and 7-AAD (BD Pharmingen, San Diego, CA.), and then analyzed with flow cytometry.

Immunohistchemical

Immunohistochemical (IHC) staining of HLA class I, TTK, URLC10, KOC1, VEGFR1 and VEGFR2 antigens of the ESCC and adjacent normal tissues were investigated using the serial sections of formalin-fixed, paraffin-embedded biopsy samples, as described previously [25]. The primary antibodies used in this study were as follows: HLA class I (Cosmo Bio. Co.Ltd. Tokyo, Japan), URLC10 (Imagenex, San Diego, CA.), TTK (Novus Bio. LLC. Littleton, CO.), KOC1 (Santacruz Bio. Inc. Dallas, Texas), VEGFR1 (Novus Bio. LLC.) and VEGFR2 (R&D Systems Inc., Minneapolis, MN). Immunoreaction was detected using the following secondary antibody systems: Simple Stain MAX-PO kit (Nichirei Bioscience, Tokyo, Japan) for HLA class I, URLC10, KOC1 and TTK; and CSA-II Biotin-free Tyramide Single Amplification System (Dako Inc., Carpinteria, CA) for VEGFR1

and VEGFR2, according to the instructions of the manufacturer. The intensity of staining was evaluated using the following criteria: strong positive staining of more than 80% (+++), positive staining of 50-80% (++); positive less than 50% (+); and no appreciable staining in tumor cells (−).

Statistical analysis

For the statistical analysis of data, JMP v9 software was used (SAS Inc.).

Results

Patients' characteristics

Between March 2008 and October 2011, 11 unresectable ESCC patients enrolled in this study. The characteristics of these patients are shown in Table 1. The patients comprised 10 males and 1 female, with a median age of 65 years (range 58-71 years). All patients were positive for HLA-A*2402. Performance status was 0 for 8 patients, 1 for 1 patient and 2 for 2 patients. The stages of ESCC were: 3 patients with stage II (No 1, 2, 7), 4 patients with stage III (No.4, 5, 6, 10) and 4 patients with stage IV (No. 3, 8, 9, 11). These patients were unresectable by reason of widespread ESCC (No 1, 2, 7), lymph node metastasis (No 2-11), adrenal gland metastasis (No.9) and lung metastasis (No 11).

Adverse events

DLT of our study was evaluated by the dose escalation schedule. The worst toxicity throughout the treatment of 2 courses of CRT and 8th vaccination was investigated in each patient (Table 2). This therapy was well-tolerated without any serious adverse events. Major toxicities were myelo-suppression and esophagus-related toxicities. Grade 3 toxicities of leucopenia, neutropenia, anemia and thrombocytopenia occurred in 54.5%, 27.3%, 27.3% and 9.1% of patients, respectively. Grade 2 toxicities of esophagitis, nausea/vomiting, diarrhea, stomatitis/pharyngitis and hypernatremia occurred in 18.2%, 18.2%, 9.1%, 27.3% and 27.3% of patients, respectively. Grade 1 local skin reactions in the peptide vaccine injection sites were observed in 81.8%. DLT of peptide vaccine was not observed in this trial.

Table 1 Patients' characteristics

Patient no.	Dose of peptides (mg)	HLA	Age (Y)	Gender	Stage*	PS**	Target organ
1	0.5	A2402	59	M	IIA	0	Primary tumor
2	0.5	A2402	58	M	IIB	0	Primary tumor
							Lymph node
3	0.5	A2402	69	F	IVA	1	Primary tumor
							Lymph node
4	1.0	A2402	64	M	III	2	Primary tumor
							Lymph node
5	1.0	A2402	65	M	III	2	Primary tumor
							Lymph node
6	1.0	A2402	61	M	III	0	Primary tumor
							Lymph node
7	3.0	A2402	70	M	IIB	0	Primary tumor
							Lymph node
8	3.0	A2402	63	M	IVA	0	Primary tumor
							Lymph node
9	3.0	A2402	67	M	IVB	0	Primary tumor
							Lymph node
							Adrenal gland
10	3.0	A2402	71	M	III	0	Primary tumor
							Lymph node
11	3.0	A2402	67	M	IVB	0	Primary tumor
							Lymph node
							Lung

*Stage according to the TNM classification for esophageal cancer (UICC).
**PS: Performance status (ECOG).

Table 2 Summary of adverse events

Toxicity	Peptide									Total patients (n = 11)		
	0.5 mg (n = 3)			1.0 mg (n = 3)			3.0 mg (n = 5)					
	Grade*			Grade			Grade			Grade (%)		
	1	2	3	1	2	3	1	2	3	1	2	3
Dermatology/skin												
Reaction at the injection site	2	0	0	3	0	0	4	0	0	9 (81.8)	0 (0.0)	0 (0.0)
Hematological												
Leukocyte	0	0	2	0	0	2	0	1	2	0 (0.0)	1 (9.1)	6 (54.5)
Neutrocyte	0	1	1	0	1	1	0	2	1	0 (0.0)	4 (36.4)	3 (27.3)
Hemoglobin	1	1	1	1	1	1	1	1	1	3 (27.3)	3 (27.3)	3 (27.3)
Platelet	1	0	0	0	0	1	3	0	0	4 (36.4)	0 (0.0)	1 (9.1)
Non-hematological												
Esophagitis	0	1	0	2	0	0	2	1	0	4 (36.4)	2 (18.2)	0 (0.0)
AST	1	0	0	1	0	0	0	0	0	2 (18.2)	0 (0.0)	0 (0.0)
ALT	0	0	0	0	0	0	1	0	0	1 (9.1)	0 (0.0)	0 (0.0)
Creatinine	0	0	0	0	0	0	0	0	0	0 (0.0)	0 (0.0)	0 (0.0)
Nausea/vomiting	1	0	0	0	1	0	0	0	0	1 (9.1)	2 (18.2)	0 (0.0)
Diarrhea	0	1	0	0	0	0	0	0	0	0 (0.0)	1 (9.1)	0 (0.0)
Stomatitis/pharyngitis	0	1	0	0	1	0	0	1	0	0 (0.0)	3 (27.3)	0 (0.0)
Hyponatremia	0	2	0	1	0	0	1	1	0	2 (18.2)	3 (27.3)	0 (0.0)

*Adverse events were graded according to the CTCAE v3.0.

Immunohistochemical study

We evaluated the expression levels of HLA Class I, URLC10, TTK, KOC1, VEGFR1 and VEGFR2 antigens in biopsy samples of the enrolled patients (Table 3). HLA class I antigen was strong expressed in cell membrane of tumor cells of all cases. The strong expressions of URLC10, TTK and KOC1 antigens were observed in cytoplasm of tumor cells of all patients. The expressions of VEGFR1 and VEGFR2 were observed in tumor cells and stromal vessels of the ESCC tissues of all patients. Representative IHC staining of these antigens in case 6 is shown in Figure 1. Strong expressions of URLC10, TTK, KOC1 and MHC class I antigens were observed in the tumor cells. Expressions of approximately the same intensity of VEGFR1 and VEGFR2 were observed in the tumor cells and stromal vessels of the ESCC tissues.

In the adjacent normal esophageal tissues, no staining of these antigens was observed (data not shown).

Table 3 Immunohistochemical staining to each antigen of ESCC tissues

Patients no.	Immunohistochemistry*					
	HLA class I	URLC10	TTK	KOC1	VEGFR1	VEGFR2
1	+++	+++	+++	+++	++	+
2	+++	+++	+++	+++	++	++
3	+++	+++	++	+++	+	+
4	+++	+++	++	+++	++	++
5	+++	+++	+++	+++	++	+
6	+++	+++	+++	+++	+	++
7	+++	+++	+++	+++	++	++
8	+++	+++	++	+++	+	+
9	+++	+++	+++	+++	++	++
10	+++	+++	+++	+++	+	+
11	+++	+++	+++	+++	++	++

*(+++): strong positive staining of more than 80%.
(++): positive staining of 50-80%, (+): positive less than 50%.
(–): no appreciable staining.

Peptide-specific CTL responses

An IFN-γ ELISPOT assay was evaluated using PBMC periodically obtained from patients to assess the cellular immune responses to 5 kinds of peptides. Additional file 2: Table S1 shows the CTL responses to each peptide before and after the 4^{th}, 8^{th}, 12^{th} and 16^{th} vaccination, and Table 4 shows a summary of the CTL positive rates at each vaccination point. All patients showed peptide-specific CTL responses in at least one of the 5 kinds of peptide antigens during the vaccination. In these peptides, URLC10 showed the highest CTL positive rates. They were 70.0% at the 4^{th} vaccination point, 54.5% at the 8^{th} vaccination point, and 100% at the 12^{th} and 16^{th} vaccination points. CTL positive rates of the other

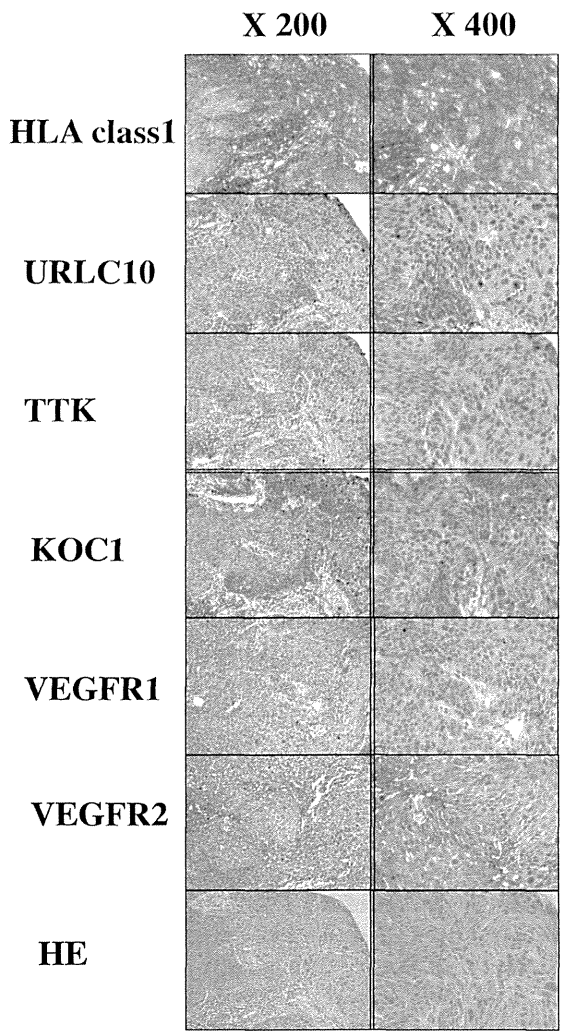

Figure 1 Immunohistochemical staining of HLA class I, URLC10, TTK, KOC1, VEGFR1 and VEGFR2 antigens in the ESCC tissues. *Typical expression of HLA class I, URLC10, TTK, KOC1, VEGFR1 and VEGFR2 in the primary ESCC tissues obtained from case 6 are shown. The staining was undertaken using the serial sections of the biopsy sample.*

peptides after vaccination, were 27.3- 40.0% for TTK, 45.5-60% for KOC1, 33.3-60% for VEGFR1, and 36.4-80.0% for VEGFR2, respectively. Furthermore, the average peptide numbers per patient which induced CTL on 8th vaccinations were 0.7 in 0.5 mg, 1.3 in 1.0 mg and 3.4 in 3.0 mg peptide administration (Table 5). Three mg of peptide induced peptide-specific CTLs more effectively than the 0.5 mg and 1 mg.

Figure 2 shows the representative data from ELISPOT assays against URLC10 in case 6 at the 8th vaccination point. URLC10-specific T cell responses were observed in PBMC derived from patient (Figure 2a, b). Moreover, the peptide-specific CD8 (+) T cells in the cultured T cells were confirmed by the flow cytometry, and 6.93% URLC10 dextramer positive cells were confirmed in the $CD8^+CD3^+CD4^-$ T cells (Figure 2c).

Clinical outcome

The clinical responses at the time of the 8th peptide vaccination and latest diagnosis points were evaluated according to the RECIST and are summarized in Table 6. At the time of the 8th peptide vaccination in combination with CRT, 6 patients achieved CR (stage II: No. 1, 2, 7; stage III: No.5, 6, 10), and 5 patients revealed PD (stage III: No. 4; stage IV: No. 3, 8, 9, 11). The CR rates were 100% (3/3) in stage II, 75% (3/4) in stage III and 0% (0/4) in stage IV. Furthermore, after that, 6 CR patients were continuously administered the 5 peptide vaccines, once every 2 weeks for 1 year and once a month after that until PD. Five of these 6 patients continued the CR with no evidence of disease for 4.5 years (No. 1), 4.6 years (No. 2), 2.9 years (No. 6), 2.0 years (No.7) and 1.1 years (No.10), and are still alive. Five patients died within 1 year, and 1 patient died within 2 years. Figure 3 shows the representative endoscopic appearance and computed tomography (CT) scan images of the primary cancer and CT scan images of the lymph node in the CR patients (case 6). Complete tumor regression of the primary tumor site (Figure 3c) and lymph node (Figure 3d) were observed after the treatment of the 8th peptide vaccinations with CRT.

Table 4 Summary of positive rates of CTL responses to each peptide antigen

Positive rates of CTL responses to each antigen in all patients (n = 11)						
Number of vaccination	**URLC10 (%)**	**TTK (%)**	**KOC1 (%)**	**VEGFR1 (%)**	**VEGFR2 (%)**	**CMV (%)**
Pre-vac.	27.3 (3/11)	36.4 (4/11)	40.0 (4/10)	20.0 (2/10)	40.0 (4/10)	100.0 (10/10)
4	70.0 (7/10)	27.3 (3/11)	45.5 (5/11)	33.3 (3/9)	45.5 (5/11)	100.0 (11/11)
8	54.5 (6/11)	36.4 (4/11)	45.5 (5/11)	45.5 (5/11)	36.4 (4/11)	100.0 (11/11)
12	100.0 (5/5)	40.0 (2/5)	60.0 (3/5)	40.0 (2/5)	80.0 (4/5)	100.0 (5/ 5)
16	100.0 (5/5)	40.0 (2/5)	60.0 (3/5)	60.0 (3/5)	80.0 (4/5)	100.0 (5/ 5)

CTL positive rates on the pre-vaccination, 4th, 8th, 12th or 16th vaccination were examined in all patients (n = 11), CR patients (n = 6) and PD patients (n = 5). When the ELISPOT Assay indicated +, ++ or +++, we judged it to be positive case. *p values.

Table 5 Number of peptides induced CTL on 8th vaccination

Patients no.	Dose of peptide (mg)	Number of peptides induced CTL	Average number of peptides per patient
1	0.5	0	0.7
2	0.5	2	
3	0.5	0	
4	1.0	1	1.3
5	1.0	1	
6	1.0	2	
7	3.0	1	3.4
8	3.0	3	
9	3.0	4	
10	3.0	5	
11	3.0	4	

*Average number of peptides per patient which induced. CTL on 8th vaccination.

Discussion

Our phase I clinical trial comprising a combination therapy of multiple-peptide vaccine and CRT in patients with HLA-A*2402 positive unresectable ESCC proceeded with satisfactory safety levels in all the patients. Peptide-specific CTL could be induced by the all peptide vaccine. In the assessment of clinical response, 6 CR and 5 PD cases were recognized, and 4 CR patients showed a prolonged survival period for 2.0-4.6 years.

The immunotherapies for unresectable or advanced ESCC patients using the peptide vaccines are of interest. Using the NY-ESO-1 peptide mixed with Picibanil OK432 and montanide ISA-51, it has been demonstrated that this peptide vaccine is able to elicite a CD4 and CD8 T cell response [26]. The usefulness of peptide vaccines TTK and URLC10 (LY6K), and KOC1 (IMP-3) have also been investigated and antigen-specific CD8 T cell responses successfully elicited in other studies [22,27]. However, the effects of these studies were limited in their clinical benefit.

In this study, we hypothesized that immunotherapy may achieve effective clearance of residual cancer cells after CRT and that this may improve the prognosis. It

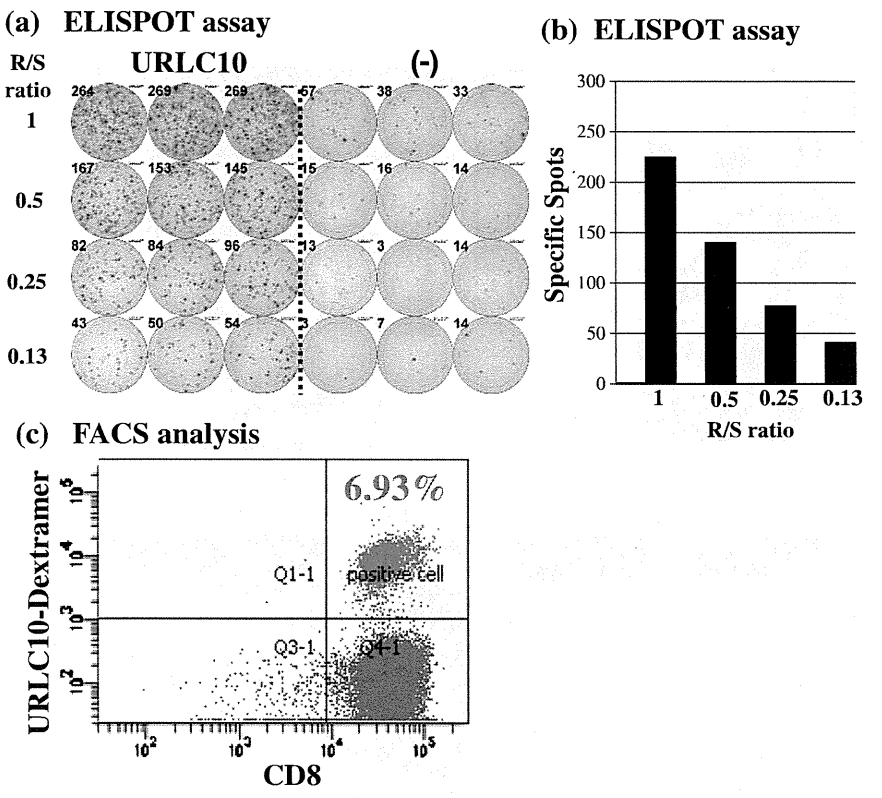

Figure 2 Representative immunological monitoring assays detecting peptide-specific CTL response. PBLs obtained from CR patient (case 6) after the 8th vaccination were cultured with URLC10-peptide stimulation and subjected to the ELISPOT assay **(a, b)**. The cultured lymphocytes were analyzed by flow cytometry, and proportion of URLC10 dextramer positive cells in $CD8^+CD3^+CD4^-$ cells were calculated **(c)**.

Table 6 Clinical responses

Patient no.	Stage	Clinical response*		Number of vac.	CR duration period (year)	PFS (days)	OS (days)	Outcome
		8^{th} vac.	Final results					
1	IIA	CR	CR	22	4.5	1659	1775	Alive
2	IIB	CR	CR	85	4.6	1681	1709	Alive
3	IVA	PD	PD	8		67	154	Dead
4	III	PD	PD	8		84	123	Dead
5	III	CR	PD	12		127	765	Dead
6	III	CR	CR	69	2.9	1072	1234	Alive
7	IIB	CR	PD	26	2.0	733	1105	Alive
8	IVB	PD	PD	10		176	231	Dead
9	IVB	PD	PD	8		59	300	Dead
10	III	CR	CR	36	1.1	384	660	Alive
11	IVB	PD	PD	15		155	217	Dead

*Clinical responses of patients were analyzed after the 8^{th} vaccination and the latest diagnosis points. CR: complete response; PD: progressive disease; PFS: Progression-free survival; OS: overall survival.

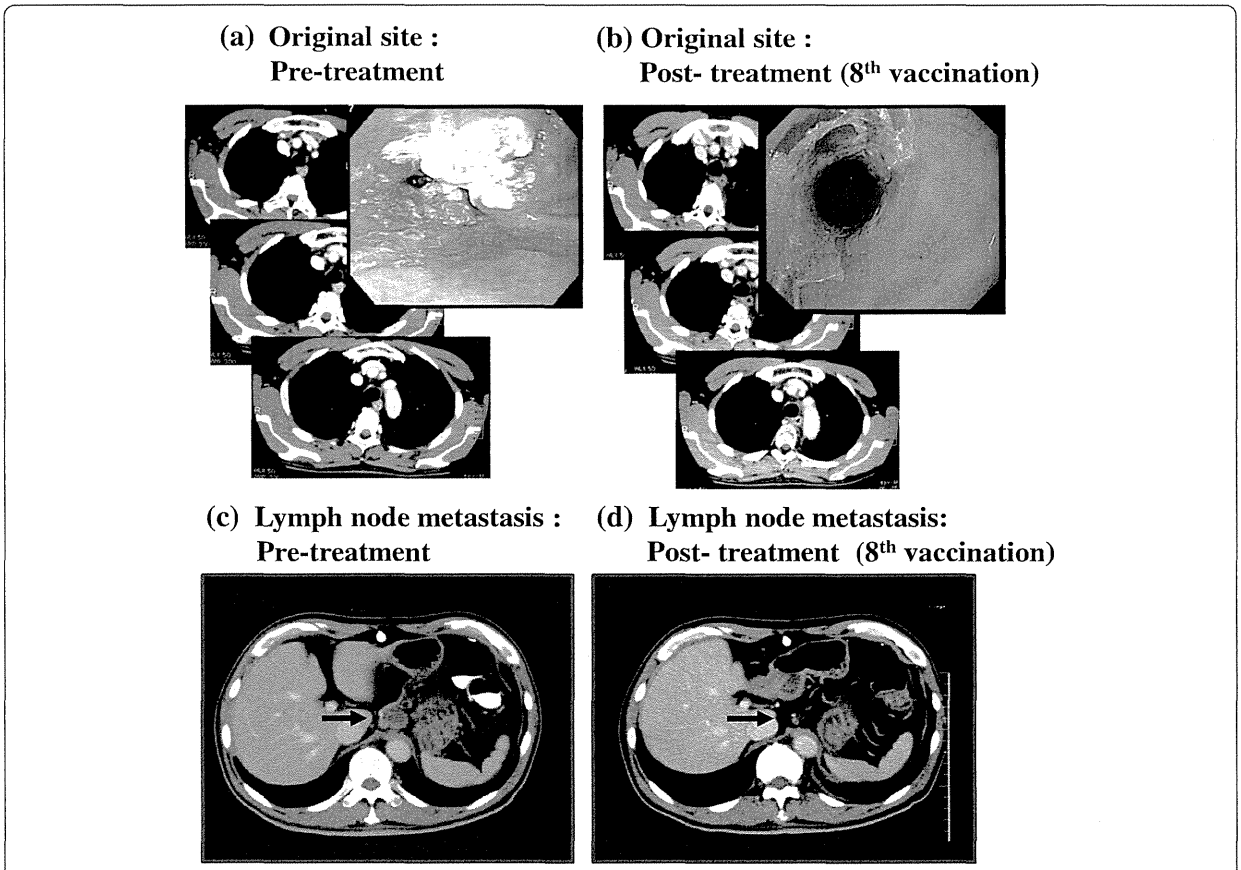

Figure 3 Computed tomography (CT) and endoscopic images of CR patient (case 6). The CT and endoscopic images of the original site **(a, b)** and CT images of lymph nodes metastasis **(c, d)** in case 6, before **(a, c)** and after treatment by CRT with 8^{th} vaccination **(b, d)** are shown.

had been thought that the main mechanism of the tumor reduction after irradiation is direct damage to tumor DNA by ionizing irradiation. Recently, however, several interesting studies have reported that local irradiation of tumor tissue elicits immunomodulation effects and inhibits tumor growth through the generation of tumor-specific CTL [28]. This concept has been supported by the accumulating data of many investigators based on basic and clinical studies [10-14,29]. Lugade et al. reported that local radiation increased both the generation of the peptide-reactive IFN-γ producing anti-tumor immune cells and their trafficking to the tumor-draining lymph nodes [10]. The essential role of $CD8^+$ T-cells in radiation therapy has been demonstrated and it has been suggested that TLR4 on host dendritic cells may be crucial role for induction of these antitumor T cells [11,13,29]. Interestingly, Aktsu et al. demonstrated that radiation itself not only kills the tumor cells but can also evoke a systemic antitumor effect (abscopal effect) by the enhancement of the heat shock protein gp96 [30]. Furthermore, many studies support the immunomodulation effects of chemotherapy. Hattori et al. demonstrated an increase of immunological responses in cases of personalized peptide vaccination combined with UFT and UZEL in metastatic colorectal cancer patients and Sato et al. reported on the usefulness of the personalized peptide vaccine in combination with TS-1 [31,32]. These results suggest that not only radiation but also some kind of anticancer drug may have potential could enhance the anti-tumor response of immunotherapy.

In contrast, clinical trials of immunotherapy combined with CRT have been few in number. Marten et al. evaluated a randomized phase II trial of adjuvant therapy of IFN-α combined with 5-FU/CDDP and radiation in patients with R0 or R1 pancreatic adenocarcinoma, and concluded that this therapy had a minor impact on the clinical response and the lowering of toxicity levels [33]. However, no study has hitherto reported a clinical trial of peptide vaccine combined with CRT in ESCC patients.

In preliminary examination, we investigated the adverse events of CRT standard regimens in Japan, with a focus on the number of lymphocytes which is the key of immunological response of tumor vaccine. Because JCOG9906 showed the less grade of lymphopenia as compared with that of other regimen, we selected this regimen for our study (Additional file 3: Table S2). In our clinical trial, we have demonstrated that our protocol was well-tolerated. Major toxicities were myelosuppression and esophagitis may be related to CRT, and grade 3 toxicities of leucopenia, neutropenia, anemia and thrombocutopenia occurred in 54.5%, 27.3%, 27.3% and 9.1% of patients, respectively. With regards to the toxicities of unresectable advanced ESCC patients treated with CRT, it was reported that grade 3 leukopenia, neutropenia, anemia and esophagitis were observed in 33.3%, 8.3%, 6.7% and 3.3% of the patients, respectively, and grade 4 platelet, dyspnea and infection were observed in 3.3%, 1.7%, and 1.7% of the patients, respectively [8]. In contrast to these studies, our protocol did not show any grade 4 hematological toxicity and non-hematological toxicity. As toxicity related to peptide vaccine, grade 1 local skin reactions at the injection sites of peptide vaccines were observed in 81.8% of patients, which is almost the same results with that of previous study of peptide vaccines for ESCC patients [25].

In the guidance of FDA for cancer vaccine, it states that the maximum tolerated dose for a cancer vaccine may not be identified except in very rare situations. Furthermore it was also described that, when no DLT is expected or achieved, optimization of other outcomes, such as the immune response, can be useful to identify doses for subsequent studies [34]. In our study, DLT was not detected in any patients. However, in a comparison of the CTL induction of 8th vaccination, we observed that the 3 mg of peptide seems to induce peptide-specific CTLs more effectively than the 0.5 mg and 1 mg levels. Therefore, we recommend that 3 mg be the basis for future study.

In this study, all biopsy samples of ESCC tissues collected from patients showed clear expressions of HLA class I antigen and all peptides antigens (URLC10, TTK, KOC1, VEGFR1, and VEGFR2). Positive rates of peptide specific CTL reactions at the 8^{th} vaccination were 54.5% for URLC10, 36.4% for TTK, 45.5% for KOC1, 45.5% for VEGFR1 and 36.4% for VEGFR2, and then increased to 40-100% at the 16^{th} vaccination. CTL positive levels for URLC10, TTK and KOC1 are almost the same as those found in previous reports which used the peptide vaccine in ESCC patients [22,23]. Regarding the mechanism of CTL production, we speculate that the apoptosis and necrosis of cancer cells by CRT may induce a pro-inflammatory response in the tumor environment, and may enhance the immunogenicity of the cancer cells and antigen presentation of DC, and that this may result in increased CTL production (Figure 4).

The clinical responses in our study were 6 CR (3 patients with stage II, 3 patients with stage III) and 5 PD (1 patient with stage III, 4 patients with stage IV). It has been reported that CRT itself showed CR at a rate of 62% (78% in the T1-2 disease and 55% in the T3 disease) [7]. However, it is known that 30-50% of patients treated with CRT recur within 1 year [4,5]. In contrast, our study showed that in 4 cases out of 6 CR patients showed a long and continuous CR period (2.0-4.6 years). This study is a phase I trial and the primary endpoint was toxicity. The patient number of this study is small

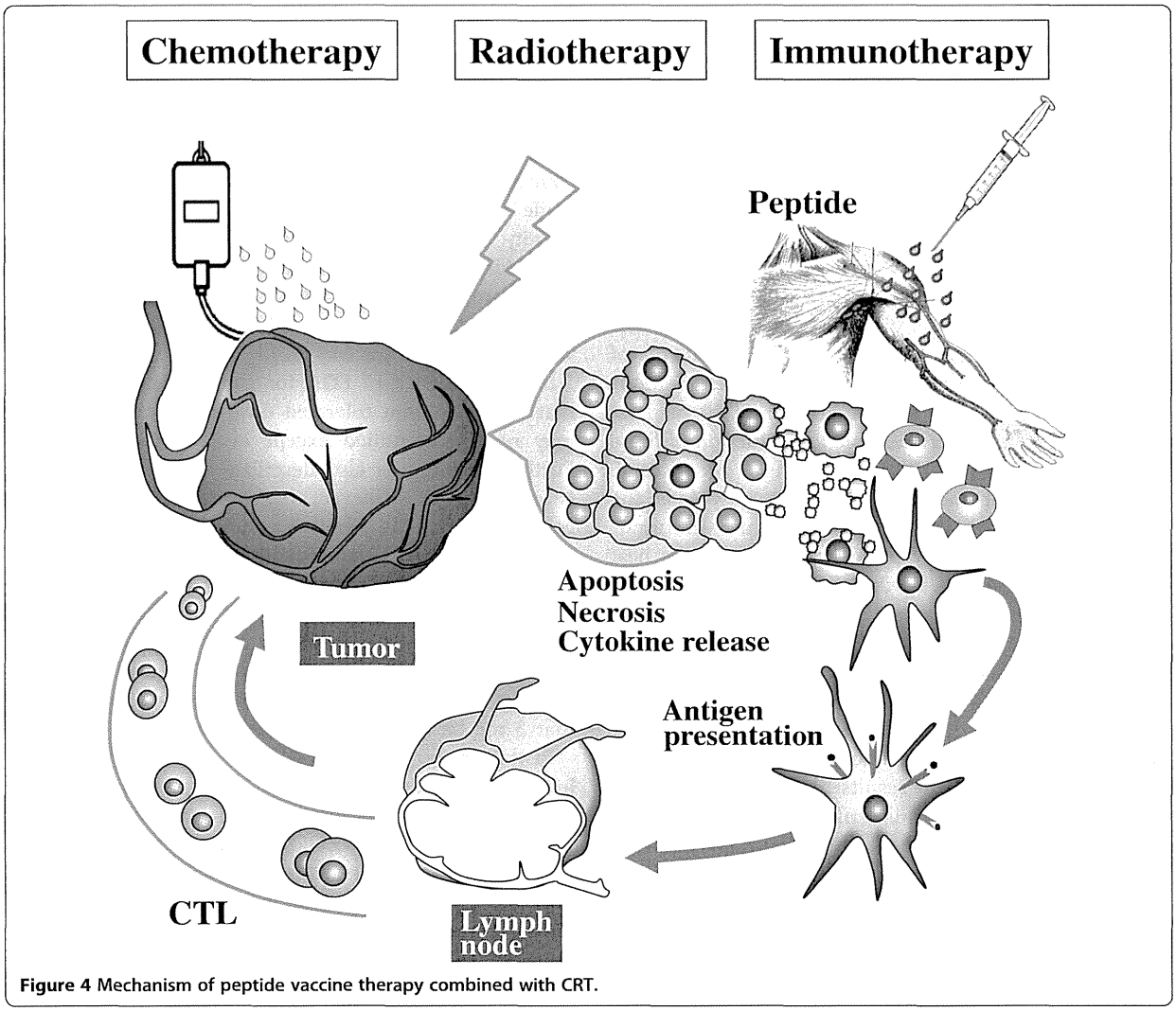

Figure 4 Mechanism of peptide vaccine therapy combined with CRT.

and we did not include the CRT patients without peptide vaccines as a comparison group. Therefore, it is difficult to clarify the clinical significance of these prolonged CR periods, at this stage. We expect that antitumor effect of peptide vaccine for residual cancer cells after CRT will become apparent in phase II trials.

Conclusions

To the best of our knowledge our study is the first clinical trial of a multi-peptide vaccine combined with CRT that has demonstrated the safety and induction of peptide specific CTL followed by a long CR period in unresectable ESCC patients. Our results point to the need to move forward to the next-stage of this combination therapy in an adjuvant setting of ESCC patients.

Additional files

Additional file 1: Figure S1. Treatment protocol.

Additional file 2: Table S1. Peptide antigen-specific CTL responses in PBLs evaluated by ELISPOT assay.

Additional file 3: Table S2. Comparison of toxicities in two regimens of CRT.

Abbreviations

ESCC: Esophageal squamous cell carcinoma; CRT: Chemoradiation therapy; TTK: TTK protein kinase; URLC10: Up-regulated lung cancer 10; KOC1: Insulin-like growth factor–II mRNA binding protein 3; VEGFR1: Vascular endothelial growth factor receptor 1; VEGFR2: Vascular endothelial growth factor receptor 2; ELISPOT: Enzyme-linked immunospot; PBMC: Peripheral blood mononuclear cells; CTL: Cytotoxic T lymphocytes; CR: Complete clinical response; PD: Progressive disease; IHC: Immunohistochemical; PFS: Progression free survival.

Competing interests
K. Yoshida and T. Tsunoda are current employed (other than primary affiliation; e.g., consulting) by OncoTherapy Science, Inc. Y. Nakamura is a stockholder and scientific advisor for OncoTherapy Science, Inc. No potential conflicts of interest were disclosed by the other authors.

Authors' contributions
HI participated in the conception, design and the writing of manuscript. RF and KO participated in the design, review and revision of the manuscript. TI, JT and MH participated in the analysis and interpretation of data. KT, KY and TT participated in the immunological assay. All authors participated in the data acquisition and discussion of the manuscript. All authors read and approved the final manuscript.

Acknowledgements
This work was supported by JSPS KAKENHI Grant Number 24591984. We thank Prof. Y. Sugiyama for his helpful discussion and Dr. K. Hoshimoto for his pathological comments for IHC.

Author details
[1]Department of Surgery, Teikyo University School of Medicine, Tokyo, Japan. [2]Laboratory of Molecular Medicine, Human Genome Center, Institute of Medical Science, University of Tokyo, Tokyo, Japan. [3]OncoTherapy Science Incorporation, Research and Development Division, Kanagawa, Japan. [4]The University of Chicago, Chicago, IL, USA. [5]Department of Immunology, Juntendo University School of Medicine, Tokyo, Japan.

Received: 21 November 2013 Accepted: 13 March 2014
Published: 3 April 2014

References

1. *Cancer statistics in Japan 2013.* Edited by Editorial Board of the Cancer Statistics in Japan. Tokyo: Foundation for Promotion of Cancer Research; 2013.
2. Ando N, Iizuka T, Ide H, Ishida K, Shinoda M, Nishimaki T, Takiyama W, Watanabe H, Isono K, Aoyama N, Makuuchi H, Tanaka O, Yamana H, Ikeuchi S, Kabuto T, Nagai K, Shimada Y, Kinjo Y, Fukuda H: **Surgery plus chemotherapy compared with surgery alone for localize squamous cell carcinoma of the thoracic esophagus: a Japan clinical oncology group study–JCOG9204.** *J Clin Oncol* 2003, **21**:4592–4596.
3. Akiyama H, Tsurumaru M, Udagawa H, Kajiyama Y: **Radical lymph node dissection for cancer of the thoracic esophagus.** *Ann Surg* 1994, **220**:364–372.
4. Shitara K, Muro K: **Chemoradiotherapy for treatment of esophageal cancer in Japan: current status and perspectives.** *Gastrointest Cancer Res* 2009, **3**:66–72.
5. Ohtsu A: **Chemoradiotherapy for esophageal cancer: current status and perspective.** *Int J Clin Oncol* 2004, **9**:444–450.
6. Le Prise E, Etienne PL, Meunier B, Maddern G, Hassel MB, Gedouin D, Boutin D, Campion JP, Launois B: **A randomized study of chemotherapy, radiation therapy, and surgery versus surgery for localized squamous cell carcinoma of the esophagus.** *Cancer* 1994, **73**:1779–1784.
7. Kato K, Muro K, Minashi K, Ohtsu A, Ishikura S, Boku N, Takiuchi H, Komatsu Y, Miyata Y, Fukuda H: **Phase II study of chemoradiotherapy with 5-fluorouracil and cisplatin for stage II-III esophageal squamous cell carcinoma: JCOG Trial (JCOG 9906).** *Int J Radiat Oncol Biol Phys* 2011, **81**:684–690.
8. Ishida K, Ando N, Yamamoto S, Ide H, Shinoda M: **Phase II studyofcisplatin and 5-fluorouracil with concurrent radiotherapy in advanced squamous cell carcinoma of the esophagus: a japan esophageal oncology group (JEOG)/japan clinical oncology group trial (JCOG9516).** *Jpn J Clin Oncol* 2004, **34**:615–619.
9. Akutsu Y, Matsubara H: **Perioperative management for the prevention of postoperative pneumonia with esophageal surgery.** *Ann Thorac Cardiovasc Surg* 2009, **15**:280–285.
10. Lugade AA, Moran JP, Gerber SA, Rose RC, Frelinger JP, Lord EM: **Local radiation therapy of B16 melanoma tumors increases the generation of tumor antigen-specific effector cells that traffic to the tumor.** *J Immunol* 2005, **174**:7516–7523.
11. Apetoh L, Ghiringhelli F, Tesniere A, Obeid M, Ortiz C, Criollo A, Mignot G, Maiuri MC, Ullrich E, Saulnier P, Yang H, Amigorena S, Ryffel B, Barrat FJ, Saftig P, Levi F, Lidereau R, Nogues C, Mira JP, Chompret A, Joulin V, Clavel-Chapelon F, Bourhis J, Andre F, Delaloge S, Tursz T, Kroemer G, Zitvogel L: **Toll-like resceptor 4-dependent contribution of the immune system to anticancer chemotherapy and radiotherapy.** *Nat Med* 2007, **13**:1050–1059.
12. Apetoh L, Ghiringhelli F, Tesniere A, Criollo A, Ortiz C, Lidereau R, Mariette C, Chaput N, Mira JP, Delaloge S, Andr'e F, Tursz T, Kroemer G, Zitvogel L: **The interaction between HMGB1 and TLR4 distates the outcome of anticancer chemotherapy and radiotherapy.** *Immunol Rev* 2007, **220**:47–59.
13. Lee Y, Auh SL, Wang Y, Burnette B, Wang Y, Meng Y, Beckett M, Sharma R, Chin R, Tu T, Weichselbaum RR, Fu YX: **Therapeutic effects of ablative radiation on local tumor require CD8+ T cells: changing strategies for cancer treatment.** *Blood* 2009, **114**:589–595.
14. Chamoto K, Takeshima T, Wakita D, Ohkuri T, Ashino S, Omatsu T, Shirato H, Kitamura H, Togashi Y, Nishimura T: **Combination immunotherapy with radiation and CpG-based tumor vaccination for the eradication of radio-and immune-resistant lung carcinoma cells.** *Cancer Sci* 2009, **100**:934–939.
15. Emens LA, Jaffee EM: **Leveraging the activity of tumor vaccines with cytotoxic chemotherapy.** *Cancer Res* 2005, **65**:8059–8064.
16. Shurin GV, Tourkova IL, Kaneno R, Shurin MR: **Chemotherapeutic agents in non cytotoxic concentrations increase antigen presentation by dendric cells via in IL-12-dependent mechanisms.** *J Immunol* 2009, **183**:137–141.
17. Correale P, Aquino A, Giuliani A, Pellegrini M, Micheli L, Cusi MG, Nencini C, Petrioli R, Prete S, De Vecchis L, Turriziani M, Giorgi G, Bonmassar E, Francini G: **Treatment of colon and breast carcinoma cells with 5-fluorouracil enhances expression of carcinoembryonic antigen and susceptibility to HLA-A (*) 02.01 restricted, CEA-peptide-specific cytotoxic T cells in vitro.** *Int J Caner* 2003, **104**:437–445.
18. Suda T, Tsunoda T, Daigo Y, Nakamura Y, Tahara H: **Identification of human leukocyte antigen-A24-restricted epitope peptides derived from gene products upregulated in lung and esophageal cancers as novel targets for immunotherapy.** *Cancer Sci* 2007, **98**:1803–1808.
19. Yamabuki T, Daigo Y, Kato T, Hayama S, Tsunoda T, Miyamoto M, Ito T, Fujita M, Hosokawa M, Kondo S, Nakamura Y: **Genome-wide gene expression profile analysis of esophageal squamous cell carcinomas.** *Int J Oncol* 2006, **28**:1375–1384.
20. Wada S, Tsunoda T, Baba T, Primus FJ, Kuwano H, Shibuya M, Tahara H: **Rationale for antiangiogenic cancer therapy with vaccination using epitope peptides derived from human vascular endothelial growth factor receptor 2.** *Cancer Res* 2005, **65**:4939–4946.
21. Ishizuka H, Tsunoda T, Wada S, Yamaguchi M, Shibuya M, Tahara H: **Inhibition of tumor growth with antiangiogenic cancer vaccine using epitope peptides derived from human vasclar endothelial growth factor receptor 1.** *Clin Cancer Res* 2006, **12**:5841–5849.
22. Kono K, Mizukami Y, Daigo Y, Takano A, Masuda K, Yoshida K, Tsunoda T, Kawaguchi Y, Nakamura Y, Fujii H: **Vaccination with multiple peptides derived from novel cancer-testis antigens can induce specific T-cell responses and clinical responses in advanced esophageal cancer.** *Cancer Sci* 2009, **100**:1502–1509.
23. Kono K, Iinuma H, Akutsu Y, Tanaka H, Hayashi N, Uchikado Y, Noguchi T, Fujii H, Okinaka K, Fukushima R, Matsubara H, Ohira M, Baba H, Natsugoe S, Kitano S, Takeda K, Yoshida K, Tsunoda T, Nakamura Y: **Multicenter, phase II clinical trial of cancer vaccination for advanced esophageal cancer with three peptides derived from novel cancer-testis antigens.** *J Transl Med* 2012, **10**:141.
24. Miyazawa M, Ohsawa R, Tsunoda T, Hirono S, Kawai M, Tani M, Nakamura Y, Yamaue H: **Phase I clinical trial using peptide vaccine for human vascular endothelial growth factor receptor 2 in combination with gemcitabine for patients with advanced pancreatic cancer.** *Cancer Sci* 2010, **101**:433–439.
25. Mizukami Y, Kono K, Daigo Y, Takano A, Tsunoda T, Kawaguchi Y, Nakamura Y, Fujii H: **Detection of novel cancer-testis antigen-specific T-cell responses in TIL, regional lymph nodes, and PBL in patients with esophageal squamous cell carcinoma.** *Cancer Sci* 2008, **99**:1448–1454.
26. Kakimi K, Isobe M, Uenaka A, Wada H, Sato E, Doki Y, Nakajima J, Seto Y, Yamatsuji T, Naomoto Y, Shiraishi K, Takigawa N, Kiura K, Tsuji K, Iwatsuki K, Oka M, Pan L, Hoffman EW, Old LJ, Nakayama E: **A phase I study of vaccination with NY-ESO-1f peptide mixed with Picibanil OK-432 and montanide ISA-51 in patients with cancers expressing the NY-ESO-1 antigen.** *Int J Cancer* 2011, **129**:2836–2846.

27. Iwahashi M, Katsuda M, Nakamori M, Nakamura M, Naka T, Ojima T, Iida T, Yamaue H: **Vaccination with peptides derived from cancer-testis antigen in combination with CpG-7909 elicits strong specific CD8+ T cell response in patients with metastatic esophageal squamous cell carcinoma.** *Cancer Sci* 2010, **101**:2510–2517.
28. Kamrava M, Bernstein MB, Camphausen K, Hodge JW: **Combining radiation, immunotherapy, and antiangiogenesis agents in the management of cancer: the three musketeers of just another quixotic combination?** *Mol BioSyst* 2009, **5**:1262–1270.
29. Takeshima T, Chamoto K, Wakita D, Ohkuri T, Togashi Y, Shirato H, Kitamura H, Nishimura T: **Local radiation therapy inhibits tumor growth through the generation of tumor-specific CTL: its potentiation by combination with Th1 cell therapy.** *Cancer Res* 2010, **70**:2697–2706.
30. Akutsu Y, Matsubara H, Urashima T, Komatsu A, Sakata H, Nishimori T, Yoneyama Y, Hoshino I, Murakami K, Usui A, Kano M, Ochiai T: **Combination of direct intratumoral administration of dendritic cell and irradiation induces strong systemic antitumor effect mediated by GRP94/gp96 against squamous cell carcinoma in mice.** *Int J Oncol* 2007, **31**:509–515.
31. Hattori T, Mine T, Komatsu N, Yamada A, Itoh K, Shiozaki H, Okuno K: **Immunological evaluation of personalized peptide vaccination in combination with UFT and UZEL for metastatic colorectal carcinoma patients.** *Cancer Immunol Immunother* 2009, **58**:1843–1852.
32. Sato Y, Fujiwara T, Mine T, Shomura H, Homma S, Maeda Y, Tokunaga N, Ikeda Y, Ishihara Y, Yamada A, Tanaka N, Itoh K, Harada M, Todo S: **Immunological evaluation of personalized peptide vaccination in combination with a 5-fluorouracil derivative (TS-1) for advanced gastric or colorectal carcinoma patients.** *Cancer Sci* 2007, **98**:1113–1119.
33. Märten A, Schmidt J, Ose J, Harig S, Abe U, Münter MW, Jäger D, Friess H, Mayerle J, Adler G, Seufferlein T, Gress T, Schmid R, Büchler MW: **A randomized multicentre Phase II trial comparing adjuvant therapy in patients with interferon alpha-2b and 5-FU alone or in combination with either external radiation treatment and cisplatin (CapRI) or radiation alone regarding event-free survival-CapRI-2.** *BMC Cancer* 2009, **9**:160.
34. Guidance for Industry: *Clinical Considerations for Therapeutic Cancer Vaccines.*; 2011. http://www.fda.gov/BiologicsBloodVaccines/GuidanceComplianceRegulatoryInformation/Guidances/Vaccines/ucm182443.htm.

doi:10.1186/1479-5876-12-84
Cite this article as: Iinuma *et al.*: Phase I clinical study of multiple epitope peptide vaccine combined with chemoradiation therapy in esophageal cancer patients. *Journal of Translational Medicine* 2014 12:84.

Published OnlineFirst October 28, 2014; DOI: 10.1158/0008-5472.CAN-14-1339

Microenvironment and Immunology

Cancer Research

Natural Killer Cells Are Essential for the Ability of BRAF Inhibitors to Control BRAF^{V600E}-Mutant Metastatic Melanoma

Lucas Ferrari de Andrade[1,2], Shin F. Ngiow[2], Kimberley Stannard[2], Sylvie Rusakiewicz[3,4,5], Murugan Kalimutho[6], Kum Kum Khanna[6], Siok-Keen Tey[7], Kazuyoshi Takeda[8], Laurence Zitvogel[3,4,9,10], Ludovic Martinet[2], and Mark J. Smyth[2,11]

Abstract

BRAF^{V600E} is a major oncogenic mutation found in approximately 50% of human melanoma that confers constitutive activation of the MAPK pathway and increased melanoma growth. Inhibition of BRAF^{V600E} by oncogene targeting therapy increases overall survival of patients with melanoma, but is unable to produce many durable responses. Adaptive drug resistance remains the main limitation to BRAF^{V600E} inhibitor clinical efficacy and immune-based strategies could be useful to overcome disease relapse. Tumor microenvironment greatly differs between visceral metastasis and primary cutaneous melanoma, and the mechanisms involved in the antimetastatic efficacy of BRAF^{V600E} inhibitors remain to be determined. To address this question, we developed a metastatic *BRAF*^{V600E}-mutant melanoma cell line and demonstrated that the antimetastatic properties of BRAF inhibitor PLX4720 (a research analogue of vemurafenib) require host natural killer (NK) cells and perforin. Indeed, PLX4720 not only directly limited *BRAF*^{V600E}-induced tumor cell proliferation, but also affected NK cell functions. We showed that PLX4720 increases the phosphorylation of ERK1/2, CD69 expression, and proliferation of mouse NK cells *in vitro*. NK cell frequencies were significantly enhanced by PLX4720 specifically in the lungs of mice with BRAF^{V600E} lung metastases. Furthermore, PLX4720 also increased human NK cell pERK1/2, CD69 expression, and IFNγ release in the context of anti-NKp30 and IL2 stimulation. Overall, this study supports the idea that additional NK cell-based immunotherapy (by checkpoint blockade or agonists or cytokines) may combine well with BRAF^{V600E} inhibitor therapy to promote more durable responses in melanoma. *Cancer Res; 74(24); 7298–308. ©2014 AACR.*

Introduction

Metastatic melanoma is a skin cancer with increasing incidence rate and poor prognosis. The mean 5-year relative survival rate for metastatic melanoma is only 16% (1). Until recently, the therapeutic options for patients with advanced-stage metastatic melanoma were very limited and remained largely ineffective in improving patient's survival (1). The identification of activating point mutations of the *BRAF* gene has been a major breakthrough in the management of metastatic melanoma (2). Valine to glutamic acid substitution at codon 600 (BRAF^{V600E}) is the most common mutation present in *BRAF* gene and is approximately found in 50% of all melanoma cases (3). BRAF^{V600E} has been shown to trigger constitutive activation of the MAPK pathway, resulting in increased cell proliferation and invasiveness (2). The large proportion of patients bearing BRAF^{V600E} mutations provided a strong rationale for the development of small-molecule–based BRAF^{V600E}-selective inhibitors. Vemurafenib (PLX4032), and its research analogue PLX4720, are ATP-competitive inhibitors for BRAF^{V600E} shown to reduce the kinase activity of this protein, consequently inhibiting the MAPK pathway and cell proliferation of *BRAF*^{V600E}-mutated melanoma (4, 5). Vemurafenib demonstrated improved overall and progression-free survival rates in most patients with previously untreated BRAF^{V600E} melanoma (3, 6) and was approved in 2011 by the U.S. FDA in the treatment of late-stage or unresectable melanoma (FDA Reference ID: 3001518). However, complete and durable remissions were rarely observed and progression-free

[1]Laboratorio de Pesquisa em Células Inflamatórias e Neoplásicas Group, Universidade Federal do Paraná, Curitiba, Paraná, Brazil. [2]Immunology in Cancer and Infection Laboratory, QIMR Berghofer Medical Research Institute, Herston, Queensland, Australia. [3]Gustave Roussy Cancer Campus, Villejuif, France. [4]INSERM U1015, Villejuif, France. [5]Center of Clinical Investigations in Biotherapies of Cancer (CICBT) 1428, Villejuif, France. [6]Signal Transduction Laboratory, QIMR Berghofer Medical Research Institute, Herston, Queensland, Australia. [7]Bone Marrow Transplant Laboratory, QIMR Berghofer Medical Research Institute, Herston, Queensland, Australia. [8]Department of Immunology, Juntendo University School of Medicine, Hongo, Bunkyo-ku, Tokyo, Japan. [9]Université Paris Sud-XI, Faculté de Médecine, Le Kremlin Bicêtre, France. [10]Department of Medical Oncology, IGR, Villejuif, France. [11]School of Medicine, University of Queensland, Herston, Queensland, Australia.

Note: Supplementary data for this article are available at Cancer Research Online (http://cancerres.aacrjournals.org/).

Corresponding Author: Mark J. Smyth, Immunology in Cancer and Infection Laboratory, QIMR Berghofer Medical Research Institute, 300 Herston Road, Herston 4006, Queensland, Australia. Phone: 61-7-8345-3957; Fax: 61-7-3362-0111; E-mail: mark.smyth@qimrberghofer.edu.au

doi: 10.1158/0008-5472.CAN-14-1339

Published OnlineFirst October 28, 2014; DOI: 10.1158/0008-5472.CAN-14-1339

survival did not exceed 5 to 7 months upon treatment with BRAF inhibitors (7). Drug resistance remains to date a major factor that limits BRAF^{V600E} inhibitor clinical efficacy and the discovery of strategies overcoming adaptive resistance may have a huge impact on a patient's clinical outcome (8, 9).

BRAF^{V600E} mutation contributes to melanoma immune escape (10) and accumulating evidence indicates that the efficacy of BRAF inhibitors relies on the activation of immune components against cancer cells (11–14). BRAF inhibition was associated with a decreased production of immunosuppressive soluble factors such as IL10, VEGF, and IL6 (12, 14, 15). An enhanced expression of melanoma-associated antigens together with an increased infiltration of CD8$^+$ T lymphocytes was also observed in metastases of patients receiving BRAF inhibitors (12–14, 16). Using resistant variants of Braf^{V600E}-driven mouse melanoma and melanoma-prone mice, our group recently demonstrated that combination therapy between PLX4720 and anti-CCL2 or agonistic anti-CD137 antibodies had significant antitumor activity, suggesting that immune-based therapy represents a promising strategy to overcome BRAF inhibitor drug resistance (11, 17).

Tumor microenvironment differs greatly between visceral metastases and primary cutaneous melanoma and may directly affect antitumor immune reactions and the efficacy of BRAF^{V600E} inhibitors (18, 19). A better understanding of the antimetastatic effect of BRAF inhibitors is therefore required. In this study, using the first described mouse model for metastatic BRAF^{V600E} melanoma, we establish that natural killer (NK) cells are critical for the therapeutic effect of PLX4720 through a perforin-dependent pathway. We show that PLX4720 treatment, in the context of IL2, directly enhances mouse NK cell ERK1/2 phosphorylation, proliferation, and CD69 expression and human NK cell ERK1/2 phosphorylation, CD69 expression and IFNγ release post NKp30 ligation. Finally, we demonstrate that treatment with a low dose of IL2 improves the antimetastatic efficacy of PLX4720 providing a strong rationale for combining NK cell stimulatory agents and BRAF inhibitors in metastatic melanoma.

Materials and Methods

Cell lines

The *BRAF*^{V600E} SM1WT1 melanoma cell line has already been described (11). The LWT1 cell line was derived from SM1WT1 by the intravenous injection of 5×10^5 SM1WT1 into C57BL/6 wild type (WT) mice (Fig. 1). Both SM1WT1 and LWT1 cell lines were maintained in complete RPMI-1640 with 10% heat-inactivated FCS, 2 mmol/L glutamax, 100 U/mL penicillin, and 100 μg/mL streptomycin. The genotyping for BRAF^{V600E} was achieved as previously described (20). B16F10 cells were sourced from ATCC, cultivated in complete DMEM supplemented as above. The original B16F10 cells were short tandem repeat DNA profiled, grown to bulk, and were never passaged for more than 2 weeks. They were routinely tested for mycoplasma by MycoAlert mycoplasma detection kit (Lonza, catalog number LT07-318).

Mice

C57BL/6 WT mice were purchased either from Animal Resources Centre or Walter and Eliza Hall Institute of Medical Research (Parkville, Australia) and maintained at QIMR Berghofer Medical Research Institute (QIMR, Herston, Australia). C57BL/6 *Cd226*$^{-/-}$, *Ifng*$^{-/-}$, and *Pfp*$^{-/-}$ mice have been previously described (11) and were bred, genotyped, and maintained at the QIMR. Seven- to 12-week-old male mice were used according to the QIMR animal ethics committee.

In vitro treatment of LWT1 and B16F10

The IC_{50} of the cell lines were determined by Alamar Blue (Invitrogen, catalog number DAL1025) assay according to the manufacturer's instructions. MHC class I, Rae-1, and CD155 expression were analyzed on LWT1 or B16F10 cells after 24 hours in the presence of PLX4720 (10 μmol/L) or an equivalent amount of DMSO. Cells were then incubated with Fc blocking buffer (2.4G2 antibody) and the following fluorescence conjugated mAbs: anti-mouse- CD155 (4.42.3), Rae-1 (186107), and relevant IgG isotype controls, all from Biolegend or R&D Systems. MHC class I was detected by incubation with biotinylated anti-mouse H2K^b (AF6-88.5) or H2D^b (28-14-8), with subsequent incubation with Allophycocyanin-conjugated streptavidin, all from BD Biosciences (catalog number 554067). All antibodies were diluted in 0.5% FCS 2 mmol/L EDTA PBS. Samples were acquired on a LSR IV Fortessa Flow Cytometer (BD Biosciences). Data were analyzed on FlowJo V10 (Treestar).

Western blotting

LWT1 or B16F10 cells were treated with 2.5, 5.0, or 10.0 μmol/L of PLX4720 or equivalent amount of DMSO. Purified human and mouse NK cells were cultivated with 1 μmol/L of PLX4720 or DMSO in complete RPMI supplemented with 300 U/mL IL2. After 24 hours, cells were harvested and resuspended in RIPA lysis buffer with protease inhibitors (Roche Diagnostics GmbH), 1 mmol/L sodium orthovanadate (Sigma), and 10 mmol/L sodium fluoride. Cells were then lysed by passing them through a 25-gauge needle 10 times and centrifuged at 13,200 rpm/4°C for 20 minutes to remove cell debris. Protein concentration was determined using the bicinchoninic acid protein assay reagent (Pierce, Thermo Fisher Scientific). Each protein sample (30 μg) was resolved on SDS-polyacrylamide gels and transferred to a PROTRAN BA 83 nitrocellulose membrane (Whatman Schleicher & Schuell; Sigma). Immunodetections were performed using anti-pERK1/2Thr202/204 (D13.14.4, #4370) and ERK1/2 (137F5,#4695, Cell Signaling Technology), anti-c-MYC (Y69, #1472-1, Abcam) rabbit polyclonal antibodies were used in conjunction with an horseradish peroxidase-conjugated anti-rabbit secondary antibody (Amersham, GE Healthcare). Equal loading was assessed using β-actin (Sigma) mouse monoclonal primary antibodies. The Super Signal chemiluminescent system (Pierce, Thermo Fisher Scientific) or ECL-plus (Amersham) was used for detection. Quantification of protein-band intensities by densitometric analysis was performed using NIH ImageJ software (NIH, Bethesda, MD).

Published OnlineFirst October 28, 2014; DOI: 10.1158/0008-5472.CAN-14-1339

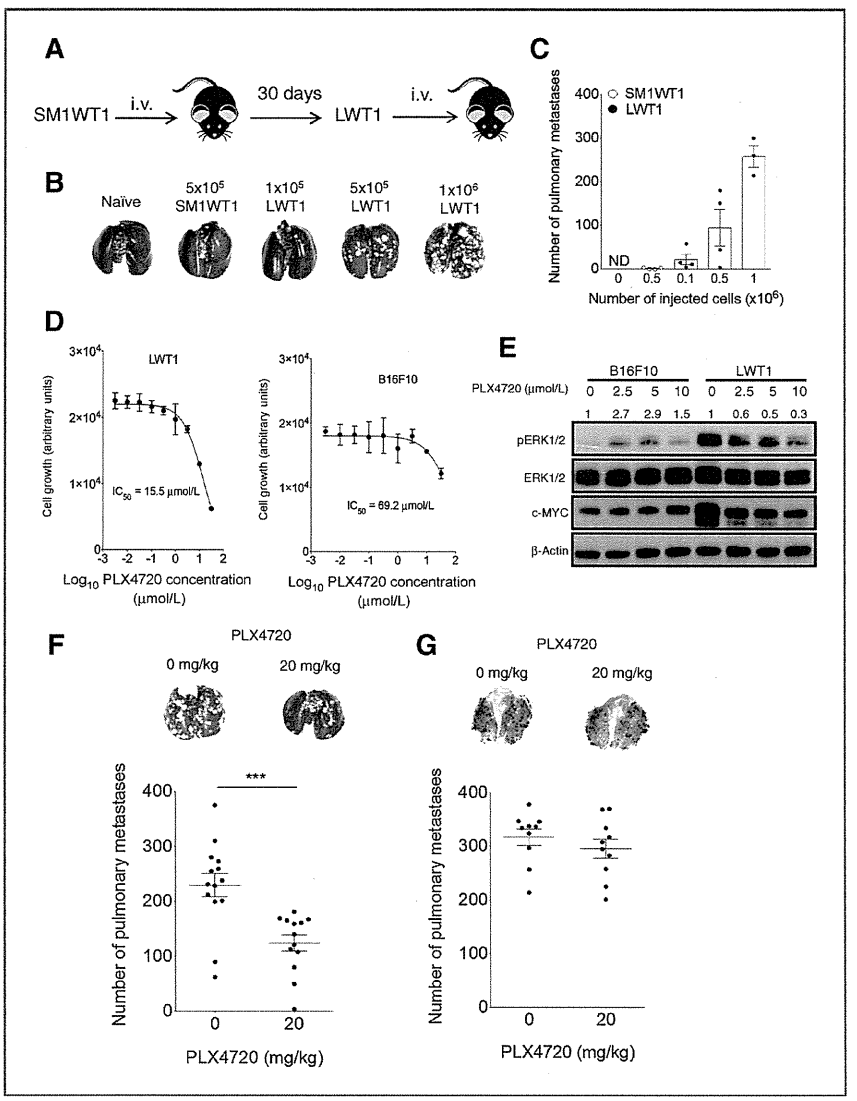

Figure 1. LWT1 is a model of metastatic $BRAF^{V600E}$ melanoma sensitive to PLX4720 inhibition. A, metastatic $BRAF^{V600E}$-mutant cell line LWT1 was generated by intravenous injection of 5×10^5 SM1WT1 cells into C57BL/6 WT mice. After 30 days, the lungs with tumor nodules were meshed through a 70-µm cell strainer and cultured as described in Materials and Methods. B and C, the indicated doses of LWT1 or SM1WT1 parental cell lines were injected intravenously in WT mice. After 14 days, lungs were harvested, perfused with India ink, and the number of metastases was counted under a microscope. B, representative pictures of lungs from each group of mice. C, graph representing the mean ± SEM number of lung metastases in the indicated group of mice. Each symbol represents one individual mouse. ND, not detected. D and E, LWT1 or B16F10 melanoma cells were treated *in vitro* with the indicated doses of PLX4720 or equivalent amount of DMSO. D, graph showing the mean ± SEM proliferation (Alamar Blue assay) of the LWT1 and B16F10 cell lines after 48 hours of culture with the indicated dose of PLX4720. Data are representative of three independent experiments. E, representative Western blot analysis with the indicated antibodies. Data are representative of three independent experiments. Fold increase in pERK1/2 relative to no PLX 4720 control is recorded above the lane. F and G, 5×10^5 LWT1 (F) or 2×10^5 B16F10 (G) were injected i.v. in C57BL/6 WT mice. Mice were treated with 20 mg/kg or equivalent amount of DMSO daily from day 1 to 7. After 14 days, lungs were harvested and representative picture of lungs from each group of mice and graph representing the mean ± SEM number of lung metastases in the indicated groups of mice are shown. Pooled data from two independent experiments are shown. Each symbol representing one individual mouse. ***, $P < 0.001$ Mann–Whitney test.

Transplant model and treatments

Pulmonary metastasis assays were performed by tail vein injection of 5×10^5 LWT1 cells or 2×10^5 B16F10 cells. PLX4720 (20 mg/kg) or equivalent amount of DMSO was given daily from day 1 to day 7 relative to tumor cell inoculation by i.p. injections. To examine IL2 immunotherapy of metastases, some groups of mice received either PBS or recombinant IL2 (10,000 or 100,000 U, Chiron Corporation) from day 1 to 5.

Published OnlineFirst October 28, 2014; DOI: 10.1158/0008-5472.CAN-14-1339

Antibody depletions were performed by i.p. injections of 100 μg of control rat IgG (HRPN – BioExcell), anti-CD4 (GK1.5 - BioExcell), anti-CD8β (53.5.8 - BioExcell), anti-NK1.1 (PK136 – BioExcell), anti-IFNγ (H22 – prepared in house), anti-NKG2D (C7 – prepared in house), or anti-asialo(as)GM1 (Wako Chemicals) on days −1, 0, and 7, relative to tumor challenge. The *in vivo* immune modulatory effects of PLX4720 on spleen NK cells were tested by daily treatment with 20 mg/kg of PLX4720 or an equivalent amount of DMSO for 3 days followed by euthanasia and analysis of NK cells from spleens by flow cytometry. To visualize the LWT1 metastasis, lungs were intratracheally perfused with 30% India Ink PBS, followed by PBS wash and 24-hour incubation with Fekete's Solution. Lung photographs and metastasis counts were both performed with a Nikon SMZ745T microscope and NIS-Elements (F.4) software.

Cells preparation and flow cytometry

Spleens were meshed, filtered at 70 μm, and washed in PBS. Red blood cells were lysed by ACK buffer incubation for 1 minute. Single-cell suspensions were incubated for 15 minutes in Fc blocking buffer (2.4G2 antibody) and stained with the following fluorescence-conjugated mAbs, all diluted at 0.5% FCS 2 mmol/L EDTA PBS: anti-mouse- CD3ε (145-2C11), TCRβ (H57-597), and NK1.1 (PK136). All mAbs were purchased from Biologend or eBioscience. Samples were acquired on a LSR IV Fortessa Flow Cytometer (BD Biosciences). Data were analyzed on FlowJo V10 (Treestar).

In vitro activation of mouse and human NK cells

C57BL/6 spleen NK cells were purified by flow cytometry (Beckman Coulter MoFlo High Speed Cell Sorting) after staining with anti-CD3ε (145-2C11) and NK1.1 (PK136). NK cells were stained with 1 μmol/L Cell Trace Violet (Invitrogen) for 10 minutes at 37°C followed by FCS and PBS wash. Human peripheral blood mononuclear cells (PBMC) were prepared on a Ficoll–Paque density gradient (Amersham Biosciences AB) by centrifugation (800 × *g*, 30 minutes at room temperature) and human $CD3^-CD56^+$ NK cells were negatively selected by magnetically activated cell sorting (NK cell isolation kit II, Miltenyi Biotec) according to the manufacturer's instructions.

Mouse or human NK cells were then cultured with the indicated concentrations of PLX4720 or an equivalent amount of DMSO in complete RPMI-1640 supplemented with 300 U/mL of human recombinant IL2. The analysis of ERK phosphorylation was performed after 24 hours in both species. Mouse NK cell activation and proliferation were assessed by flow cytometry by CD69 staining (H1.2F3) and Cell Trace Violet dilution after 3 days of cultures. Human NK cell activation was analyzed by CD69 expression after 6 days of culture.

In some experiments, purified NK cells (from 9 different donors) were cultured overnight (20 hours) in complete medium (RPMI 10% plus Human AB serum, 1% penicillin/streptomycin, 2 mmol/L glutamine, 2 mmol/L sodium pyruvate) with DMSO, PLX (0.3–3.0 μmol/L) with or without IL2 (300 U/mL). NK cells were recovered, counted, and plated (5×10^4/well) in a 96-well MAXISORB cross-linking plate (Nunc) precoated with 2.5 μg/mL anti-NKp30 (clone 210847, R&D Systems) or the IgG2a isotype control. NK cells were incubated at 37°C for an additional 20 hours and the supernatants were harvested and IFNγ measured by ELISA (BD Biosciences).

^{51}Cr release cytotoxicity assay

NK cells were stimulated with 10 ng/mL of IL15/IL15R complex (eBioscience; #14-8152-80) for 48 hours in complete RPMI and used as effector cells. LWT1 or B16F10 cells were treated with 10 μmol/L of PLX4720 or equivalent amount of DMSO for 24 hours and used as target cells. The target cells were incubated with ^{51}Cr for 60 minutes, washed in PBS, and 1,000 cells dispensed in 96-well V bottom plates. Effector cells were plated at an effector: target ratio of 1:1, 5:1, and 10:1, and incubated at 37°C for 4 hours. When indicated rat IgG (HRPN – BioExcell, 10 μg/mL), or anti-CD226 (480.1 – BioExcell, 10 μg/mL) was used in the assay. ^{51}Cr release in the supernatant was determined by reading on a Wallac 1470 WIZARD Gamma Counter and the % of killing calculated by the following equation: % specific killing = (sample cpm − spontaneous release)/(maximum release − spontaneous release) × 100.

Statistical analysis

Statistical analysis was achieved using GraphPad Prism 6 software. Unpaired Mann–Whitney test or Student *t* test was used for comparison between groups with statistical significance when *P* values were below or equal to 0.05 (*), 0.01 (**), or 0.001 (***).

Results

LWT1 is a model of metastatic BRAF^{V600E} melanoma sensitive to PLX4720 inhibition

In the absence of immune-competent BRAF^{V600E} melanoma models, the mechanisms involved in antimetastatic efficacy of BRAF^{V600E}-specific inhibitor PLX4720 remain unknown. We therefore derived an experimental metastatic cell line from the previously described BRAF^{V600E} SM1WT1 melanoma (11, 20) by intravenous passage through the lungs of a wild-type (WT) mouse (Fig. 1A). This metastatic melanoma cell line, termed LWT1, induced in 2 weeks the consistent formation of metastatic colonies restricted to the lungs in a dose-dependent manner, whereas the injection of an equal number of parental cell line SM1WT1 did not (Fig. 1B and C). Consistent with previous results obtained with the parental cell line SM1WT1 (11), we found that PLX4720 had modest activity against LWT1 (somewhat PLX4720 resistant; IC_{50} = 15.5 μmol/L), whereas PLX4720 had little detectable effect on BRAF^{wt} melanoma cell line B16F10 (IC_{50} = 69.2 μmol/L; Fig. 1D). ERK1/2 was constitutively phosphorylated in the LWT1 BRAF^{V600E} cell line and treatment with PLX4720 for 24 hours produced a dose-dependent reduction in the phosphorylation of ERK1/2 (Fig. 1E). This was associated with a decrease in c-Myc expression, a downstream target of ERK1/2 involved in cell proliferation (4), confirming the inhibition of the MAPK pathway by PLX4720 (Fig. 1E). In

Published OnlineFirst October 28, 2014; DOI: 10.1158/0008-5472.CAN-14-1339

contrast, the basal level of ERK1/2 phosphorylation was very low in $BRAF^{wt}$ B16F10 tumors but low concentrations of PLX4720 slightly increased the phosphorylation of ERK1/2 and had no impact on c-Myc expression (Fig. 1E). These data confirm the findings of previous reports showing that PLX4720 promotes the phosphorylation of ERK in $BRAF^{WT}$ melanoma cells (21, 22). We then tested the antimetastatic effect of PLX4720 *in vivo* and it was able to reduce the quantity of pulmonary metastatic foci of LWT1 by approximately 50% (Fig. 1F), while it did not affect the number of B16F10 metastases (Fig. 1G). PLX4720 was superior to either anti-CTLA-4 or anti-PD-1 treatment alone and enabled enhanced survival in this model (Supplementary Fig. S1). These results show in a metastatic context that PLX4720 has specific antimetastatic effects against $BRAF^{V600E}$ melanoma cell lines.

PLX4720 control of pulmonary LWT1 metastasis is NK cell dependent

Given the accumulating evidence showing the ability of BRAF inhibitors to modulate antimelanoma immune reactions, we analyzed the role of immune components in PLX4720 antimetastatic properties *in vivo*. PLX4720 greatly reduced the number of metastases in the lungs of Ig-treated mice as compared with DMSO-treated group (Fig. 2A and B). Similar reduction with PLX4720 was observed in mice depleted with both CD4 and CD8 mAbs (Fig. 2B). In contrast, we found that this drug had no detectable antimetastatic effect in NK cell-depleted mice (Fig. 2A and B). The role of NK cells in PLX4720 efficacy was subsequently validated using another antibody to deplete NK cells (anti-NK1.1; PK136; Fig. 2B). The antimetastatic effect of PLX4720 was lost in mice depleted of NK cells even at a lower dose of LWT1 tumor cells (Supplementary Fig. S2). These results demonstrated that the antimetastatic effects of PLX4720 relied not only on the intrinsic inhibition of melanoma cell proliferation, but also required the action of host NK cells.

Antimetastatic effect of PLX4720 depends on NK cell-mediated cytotoxicity

We next evaluated the importance of effector pathways in PLX4720-driven NK cell-mediated control of LWT1 lung metastasis. We observed that PLX4720 was still effective in mice neutralized for IFNγ or in mice deficient for IFNγ ($^{-/-}$), suggesting that the IFNγ pathway was not required for PLX4720 efficacy in *vivo* in this mouse tumor model (Fig. 3A). In contrast, mice deficient in perforin ($Pfp^{-/-}$) alone or additionally neutralized for IFNγ were unable to control LWT1 metastasis when treated with PLX4720 (Fig. 3A). These results suggested that in the LWT1 tumor model, perforin played a major role in controlling the antimetastatic efficacy of PLX4720.

NK cell release of cytotoxic granules is controlled by the integration of signals received by a wide set of activation and inhibitory receptors (23, 24). We could not detect Rae-1 family ligands while CD155 was highly expressed on LWT1 cells (Fig. 3B). In contrast, the expression of MHC-I molecules H2-K^b and $H2D^b$ was low at the cell surface of LWT1 cells (Fig. 3B). In

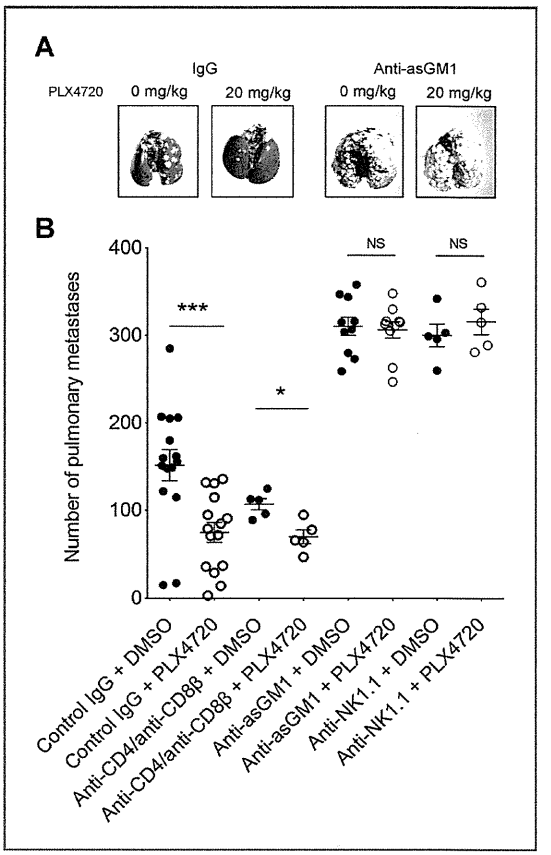

Figure 2. Antimetastatic effects of PLX4720 require NK cells. C57BL/6 WT mice were injected with the indicated depleting antibodies and were challenged intravenously with 5×10^5 LWT1 melanoma cells. Mice were subsequently treated with 20 mg/kg or equivalent amount of DMSO daily from day 1 to 7. After 14 days, lungs were harvested and perfused with India ink and lung metastases were counted under a microscope. A, representative pictures of lungs from the indicated group of mice. B, graph representing the mean ± SEM numbers of lung metastases in the indicated group of mice. Pooled data from two independent experiments are shown. Each symbol represents one individual mouse. NS, nonsignificant, $P > 0.05$; *, $P < 0.05$; ***, $P < 0.001$ Mann–Whitney test.

accordance with the low density of MHC-I and the presence of CD226 ligands, we found that LWT1 was well killed by activated NK cells in 4-hour classical ^{51}Cr assays (Fig. 3C). Interestingly, the presence of anti-CD226 antibodies in the assay was able to limit LWT1 killing, suggesting that the CD226 interaction with CD155 is important for NK cell recognition of LWT1 (Fig. 3C).

Therefore, using gene-targeted mice for CD226 ($Cd226^{-/-}$), we tested the role of these receptors in PLX4720-driven NK cell-mediated control of LWT1 lung metastasis. We found that the effect of PLX4720 was partially compromised in $Cd226^{-/-}$ mice (Fig. 3D). Additional neutralization of NKG2D did not further abrogate the activity of PLX4720 (Fig. 3D). Altogether, our

Published OnlineFirst October 28, 2014; DOI: 10.1158/0008-5472.CAN-14-1339

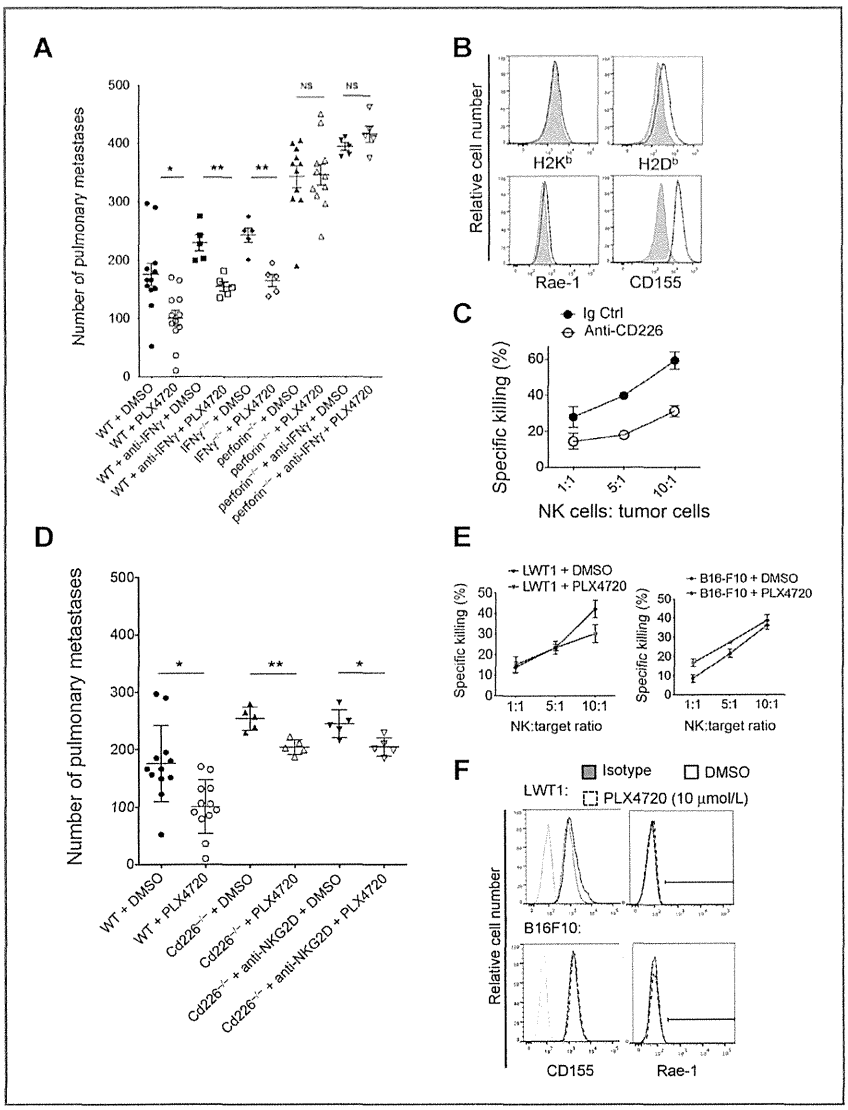

Figure 3. PLX4720 requires perforin and CD226 for optimal antimetastatic activity. A and D, the indicated strains of mice were challenged intravenously with 5×10^5 LWT1 melanoma cells and subsequently treated with 20 mg/kg or equivalent amount of DMSO daily on days 1 to 7. Antibody neutralization was performed on days −1, 0, and 7 relative to tumor challenge. After 14 days, lungs were perfused with India ink and metastases were counted under a microscope. A and D, the mean ± SEM number of lung metastases in the indicated groups of mice are shown. Data are pooled from two independent experiments. Each symbol represents an individual mouse. B, LWT1 cells were stained with antibodies against the indicated extracellular proteins and analyzed by flow cytometry. The gray histograms represent isotype controls, whereas the black lines represent the test staining. C, LWT1 cells were ^{51}Cr-labeled followed by 4 hours of coculture with activated NK cells in the presence of Ig control or anti-CD226 antibodies. Graph represents the mean ± SD of experimental replicates. Data are representative of three independent experiments. E and F, LWT1 and B16F10 cells were treated *in vitro* with 10 μmol/L of PLX4720 or equivalent amount of DMSO for 24 hours. Cells were either labeled ^{51}Cr and used as target in a cytotoxicity assay (E) or analyzed by flow cytometry for Rae-1 and CD155 expression (F). E, NK cells were activated *in vitro* for 48 hours with media supplemented with 10 ng/mL IL15/IL15Rα followed by 4 hours of incubation with PLX4720 or DMSO-treated B16F10 or LWT1 cells. Data are representative of three independent experiments. Graphs show mean ± SD of three experimental replicates. NS $P > 0.05$; *, $P < 0.05$; **, $P < 0.01$; Mann–Whitney test.

results show that the antimetastatic effects of PLX4720 require both perforin-mediated cytotoxicity and in part, tumor recognition via CD226.

To test whether PLX treatment of tumor cells increased LWT1 sensitivity to NK cell-mediated killing, LWT1 or B16F10 was cultured *in vitro* in the presence of 10 μmol/L of PLX4720